Electronic Supplementary Information

Splitting and Reorientation of π-Conjugation by an Unprecedented Photo-Rearrangement Reaction

Yuya Inaba, Tomoki Yoneda, Yuichi Kitagawa, Kiyoshi Miyata, Yasuchika Hasegawa and Yasuhide Inokuma*

Table of contents

I. General Information

Solvents and reagents were purchased from WAKO Pure Chemical Industries Ltd. and TCI Co., Ltd. and used without further purification unless otherwise mentioned. Compound **1**[1], **2**[2] and **4**[1] were prepared according to the reported procedure. All the ^{1}H and ^{13}C NMR spectra were recorded using a JEOL JMN-ECS400 spectrometer. Chemical shifts are reported in parts per million (ppm) relative to tetramethylsilane (δ = 0.00 ppm) for ^{1}H NMR and $CDCl_3$ (δ = 77.16 ppm) for ^{13}C NMR. Infrared spectra were measured using a JASCO Co. FT/IR-4600 spectrometer. Thin layered chromatography (TLC) was performed on a silica gel sheet, MERCK silica gel 60 F_{254}. Preparative thin layered chromatography was performed on a silica gel plate, Silicagel 70 PF_{254} Plate-*Wako*. Preparative scale separations were carried out using silica gel gravity column chromatography (Wakosil® 60. 64 ~ 210 μm). UV/Vis absorption spectra were recorded on a Shimadzu UV-1800 spectrophotometer. DFT calculations were performed using Gaussian 09[3] software. The photoreaction was performed using NIKKI NLSS15BM-AC LED light (9W) and SIGMAKOKI SCF-50S-42L (cut-off filter). HPLC chromatograms were recorded using a JASCO MD-2018 photodiode array detector equipped with a JASCO PU-2089 pump, JASCO AS-2059 sampler, JASCO CO-2060 column thermostat, ADVANTEC CHF 122SC fraction collector. CD spectra were recorded using a JASCO J-1500 CD spectrometer. Single crystal X-ray diffraction data were collected by a Rigaku XtaLAB P200 diffractometer equipped with a PILATUS200K detector using a multi-layer mirror (MoKα radiation λ = 0.71073 Å). All structures were solved using a dual-space algorithm (SHELXT[4]) and refined using full-matrix least-squares method (SHELXL[5]). Emission spectra were recorded on a HORIBA Fluorolog-3 spectrofluorometer and corrected for the response of the detector system. Quantum yields were measured using an FP-6300 spectrofluorometer with an integration sphere. Fluorescence lifetimes were recorded on a picosecond fluorescence lifetime measurement system (C11200, Hamamatsu) equipped with picosecond light pulser (C10196), spectrograph (C11119–02), and streak scope (C10627).

II. Synthetic Procedures

2-1. Synthesis of 3

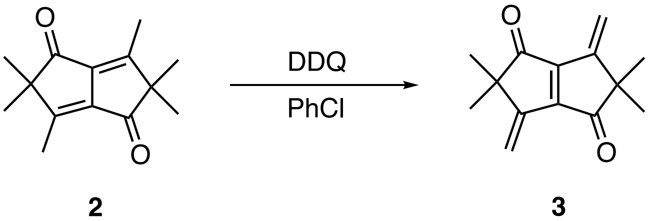

2 **3**

In a 200 mL round-bottomed flask equipped with a reflux condenser, compound **2** (1.00 g, 4.58 mmol) and 2,3-dichloro-5,6-dicyano-p-bonzoquinone (DDQ) (2.08 g, 9.16 mmol) were dissolved in chlorobenzene (100 mL), and the solution was heated to reflux for 10 h with magnetic stirring. After cooled to room temperature, the reaction mixture was filtered with suction and the residue was washed with 30 mL of chlorobenzene. The filtrate was concentrated under reduced pressure. The resulting solid was dissolved in 50 mL of ethyl acetate and washed with water (50 mL × 2), saturated aqueous solution of sodium bicarbonate (50 mL × 4), and then brine (50 mL × 2). The organic layer was dried over anhydrous sodium sulfate and concentrated under reduced pressure. The crude product was then purified by silica gel column chromatography (diameter 4.0 cm, height 20 cm, eluent: hexane/ethyl acetate = 20:1) to give 0.76 g (3.51 mmol, 76% yield) of compound **3** as a yellow solid.

^{1}H NMR (400 MHz, $CDCl_3$, 298 K): δ=5.93 (s, 2H, methylene), 5.35 (s, 2H, methylene), 1.28 (s, 12H, dimethylmethylene); ^{13}C NMR (100 MHz, $CDCl_3$, 298 K): δ=206.0 (C=O), 157.0 (C=C), 146.2 (C=C), 112.8 (C=C), 54.6 ($C(CH_3)_2$), 23.9 (CH_3); IR (ATR, neat): 2963, 2926, 2866, 1703, 1464, 1453, 1422, 1380, 1310, 1210, 1092, 976, 915 cm^{-1}; UV/Vis (dichloromethane): $\lambda_{max}(\varepsilon)$=236 (15900), 244 (16600), 341 nm (9900 mol^{-1} L cm^{-1}); HRMS (EI): m/z calcd for $C_{14}H_{16}O_2$: 216.1150 $[M]^+$, found 216.1151; R_f=0.30 (eluent: hexane/ethyl acetate 20:1); m.p. 147–151 ºC.

2-2. Synthesis of dimer 5 from 2

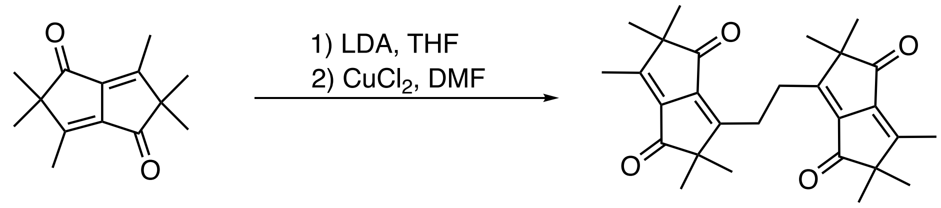

2 **5**

In a two-necked flask equipped with a dropping funnel and a gas inlet/outlet, 5.6 mL of lithium diisopropylamide (LDA) solution (1.0 M in tetrahydrofuran/hexane) was cooled to –50 ºC using cooling bath under N2 atmosphere. A solution of compound 2 (1.00 g, 4.58 mmol) in anhydrous tetrahydrofuran (8.0 mL) was added dropwise to the LDA solution keeping solution temperature at –50 ºC. After 15 min of magnetic stirring at –50 ºC, a solution of $CuCl_2$ (0.80 g, 5.95 mmol) in anhydrous *N,N*-dimethylformamide (12.0 mL) was slowly added via syringe. The reaction mixture was stirred additional 30 min at –50 ºC. Then the reaction mixture was allowed to warm to room temperature and the reaction was quenched by addition of 3% hydrochloric acid (15 mL). The mixture was extracted with dichloromethane (30 mL × 2) and washed with 3% hydrochloric acid (30 mL × 2) and water (30 mL). The organic layer was dried over anhydrous sodium sulfate and concentrated under reduced pressure. The crude product was then purified by silica gel column chromatography (diameter 4.2 cm, height 15 cm, eluent: hexane/dichloromethane/ethyl acetate = 10:1:1) to give compound 5 (0.29 g, 29% yield) as an off-white solid.

^{1}H NMR (400 MHz, $CDCl_3$, 298 K): δ=2.72 (s, 4H, ethylene), 2.11 (s, 6H, allyl methyl), 1.30 (s, 12H, dimethylmethylene), 1.21 (s, 12H, dimethylmethylene); ^{13}C NMR (100 MHz, $CDCl_3$, 298 K): δ=205.5 (*C*=O), 205.0 (*C*=O), 152.9 (*C*=C), 150.5 (*C*=C), 138.1 (*C*=C), 137.8 (*C*=C), 61.0 ($C(CH_3)_2$), 60.3 ($C(CH_3)_2$), 26.5 (CH_2), 22.2 (CH_3), 22.0 (CH_3), 11.8 (CH_3); IR (ATR, neat): 2959, 2926, 2866, 1708, 1636, 1609, 1464, 1454, 1427, 1372, 1355, 1170, 1142, 1111, 1027, 980 cm^{-1}; HRMS (ESI): *m/z* calcd for $C_{28}H_{34}O_4$+Na$^+$: 457.2349 [*M*+Na]$^+$, found: 457.2351; R_f =0.27 (eluent: hexane/ethyl acetate/dichloromethane 10:1:1); m.p. 273 – 275 ºC.

2-3. Synthetic attempt of dimer 5 from octaketone 4

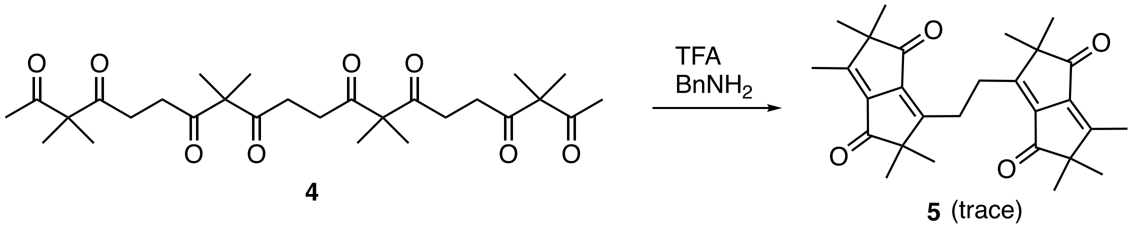

To a 10 mL round-bottomed flask equipped with a water separator (Dean-Stark apparatus) and reflux condenser, were added toluene (2.0 mL), octaketone **4** (102 mg, 0.20 mmol), benzylamine (43 µL, 0.39 mmol), and trifluoroacetic acid (36 µL, 0.47 mmol). The reaction solution was stirred under reflux for 7 h with continuous azeotropic removal of water. After the reaction mixture was cooled to room temperature, toluene (4 mL) and saturated aqueous sodium bicarbonate (4 mL) were added to the reaction mixture. The organic layer was washed with water (2 mL), dried over anhydrous sodium sulfate, and concentrated using rotary evaporator. The residue was chromatographed on a preparative thin layered silica gel plate and the fractions with R_f of 0.25–0.30 were collected. The crude product was analyzed by ^{1}H NMR spectroscopy. While formation of desired product (<1%) was confirmed by the ^{1}H NMR spectrum shown in Figure S1, compound **5** cannot be isolated from the reaction mixture.

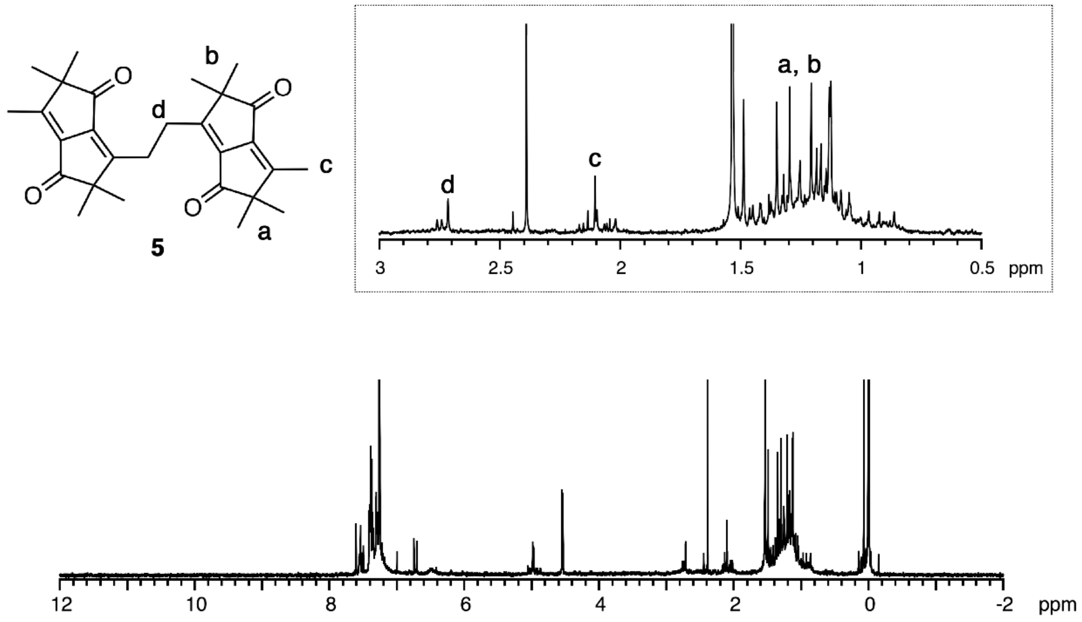

Figure S1. ^{1}H NMR spectrum of the crude reaction mixture for the synthesis of compound **5** from **4**. Inset shows the magnified spectrum and assignment of proton signals for **5**.

2-4 Synthesis of 6

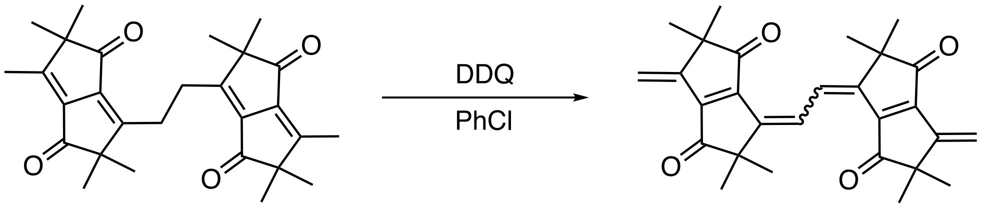

5 **6**

Compound **5** (200 mg, 0.46 mmol) and DDQ (418 mg, 1.84 mmol) were dissolved in 10 mL of chlorobenzene in a 50 mL round-bottomed flask equipped with a reflux condenser. The solution was heated to reflux for 3 h with magnetic stirring. After cooled to room temperature, the reaction mixture was filtered with suction and the residue was washed with 20 mL of chloroform. All the filtrates were collected and concentrated under reduced pressure. The resulting solid was dissolved in chloroform (30 mL) and washed with water (20 mL × 2), saturated aqueous solution of sodium bicarbonate (20 mL × 5), and then brine (20 mL × 2). The organic layer was then dried over anhydrous sodium sulfate and concentrated under reduced pressure. The crude product was column-chromatographed on silica gel (diameter 3.2 cm, height 10 cm, eluent: dichloromethane/hexane = 1:1). The resulting solid was washed with 2 mL of hexane and filtered with suction, then the solid was further washed with 1 mL of hexane to give compound **6** (106 mg, 53% yield) as a mixture of isomers (*E,E* : *E,Z* : *Z,Z* = 19:7:74) as an orange solid.

Spectroscopic data for as-obtained diastereomeric mixture of ***6***

IR (ATR, neat): 3044, 2968, 2927, 2868, 1846, 1703, 1583, 1465, 1454, 1430, 1378, 1359, 1346, 1283, 1236, 1205, 1113, 1020, 981 $\mathrm{cm^{-1}}$; UV/Vis (dichloromethane): $\lambda_{\max}(\varepsilon)$ = 305 (19600), 314 (20400), 456 nm (38100 $\mathrm{mol^{-1}\ L\ cm^{-1}}$); HRMS (APCI): *m/z* calcd for $C_{28}H_{30}O_4$: 430.2150 $[M]^-$; found; 430.2163.

*Characterization data for (Z,Z)-**6***

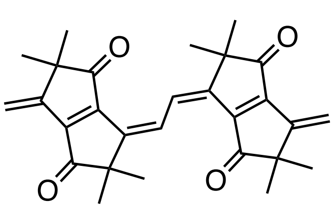

(*Z,Z*)-**6**

Recrystallization of as-obtained **6** from chloroform/ethyl acetate in the dark gave orange crystals of (*Z,Z*)-**6** exclusively.

^{1}H NMR (400 MHz, $CDCl_3$, 298 K): δ=7.89 (s, 2H, inner vinyl), 6.03 (s, 2H, terminal vinyl), 5.38 (s, 2H, terminal vinyl), 1.41 (s, 12H, dimethylmethylene), 1.32 (s, 12H, dimethylmethylene); ^{13}C NMR (100 MHz, $CDCl_3$, 298 K): δ=206.2 (*C*=O), 205.5 (*C*=O), 158.0 (*C*=C), 157.3 (*C*=C), 146.2 (*C*=C), 143.6 (*C*=C), 128.0 (*C*=C), 113.2 (*C*=C), 55.7 (*C*(CH_3)$_2$), 54.6 (*C*(CH_3)$_2$), 24.4 (*C*H_3), 24.3 (*C*H_3); R_f=0.31 (hexane/ethyl acetate 10:1).

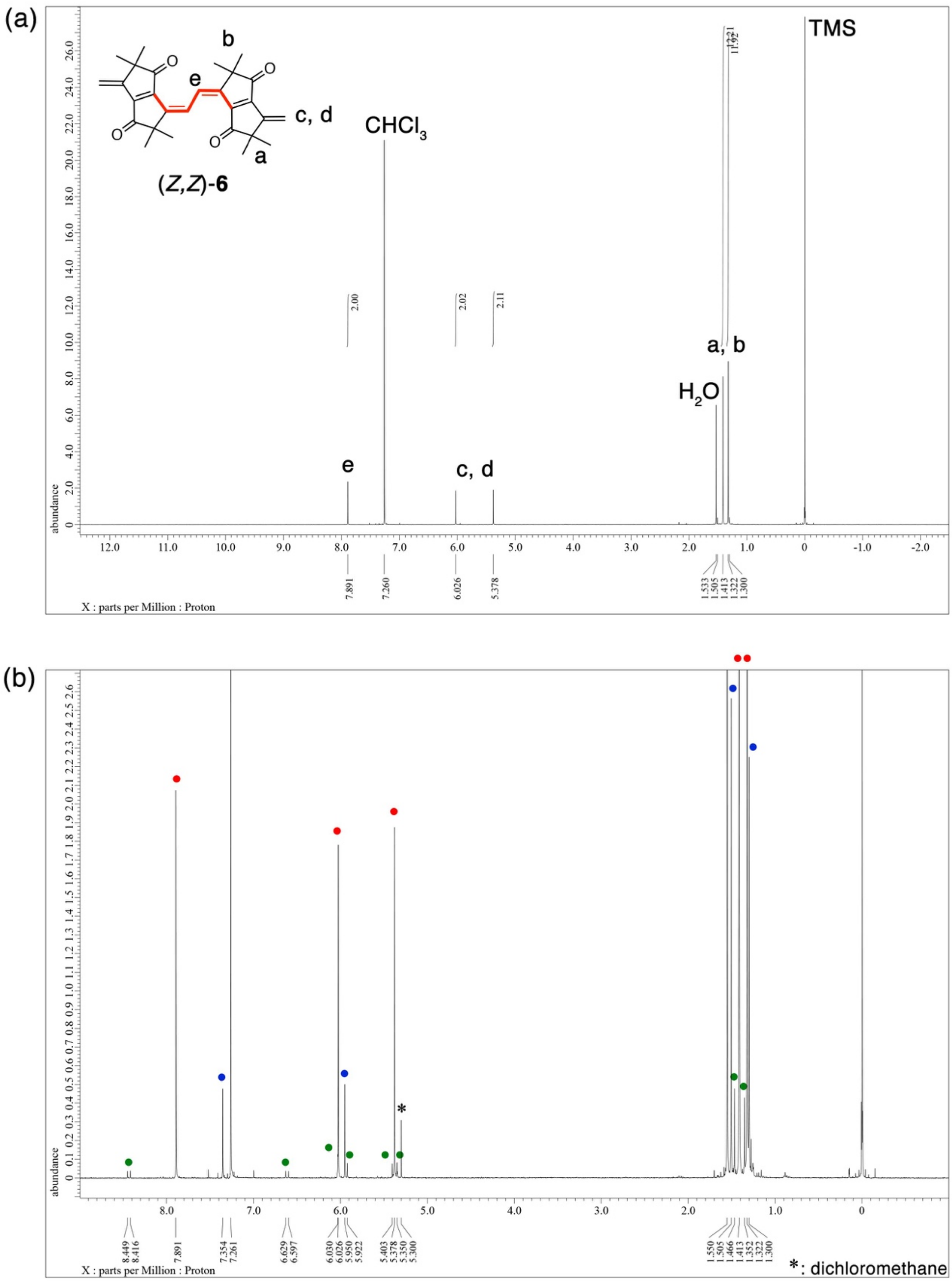

Figure S2. ^{1}H NMR spectra of (a) (*Z,Z*)-**6** and (b) as-obtained diastereomeric mixture of **6**. (Blue, green, and red dots denote *E,E*, *E,Z*, and *Z,Z* isomers)

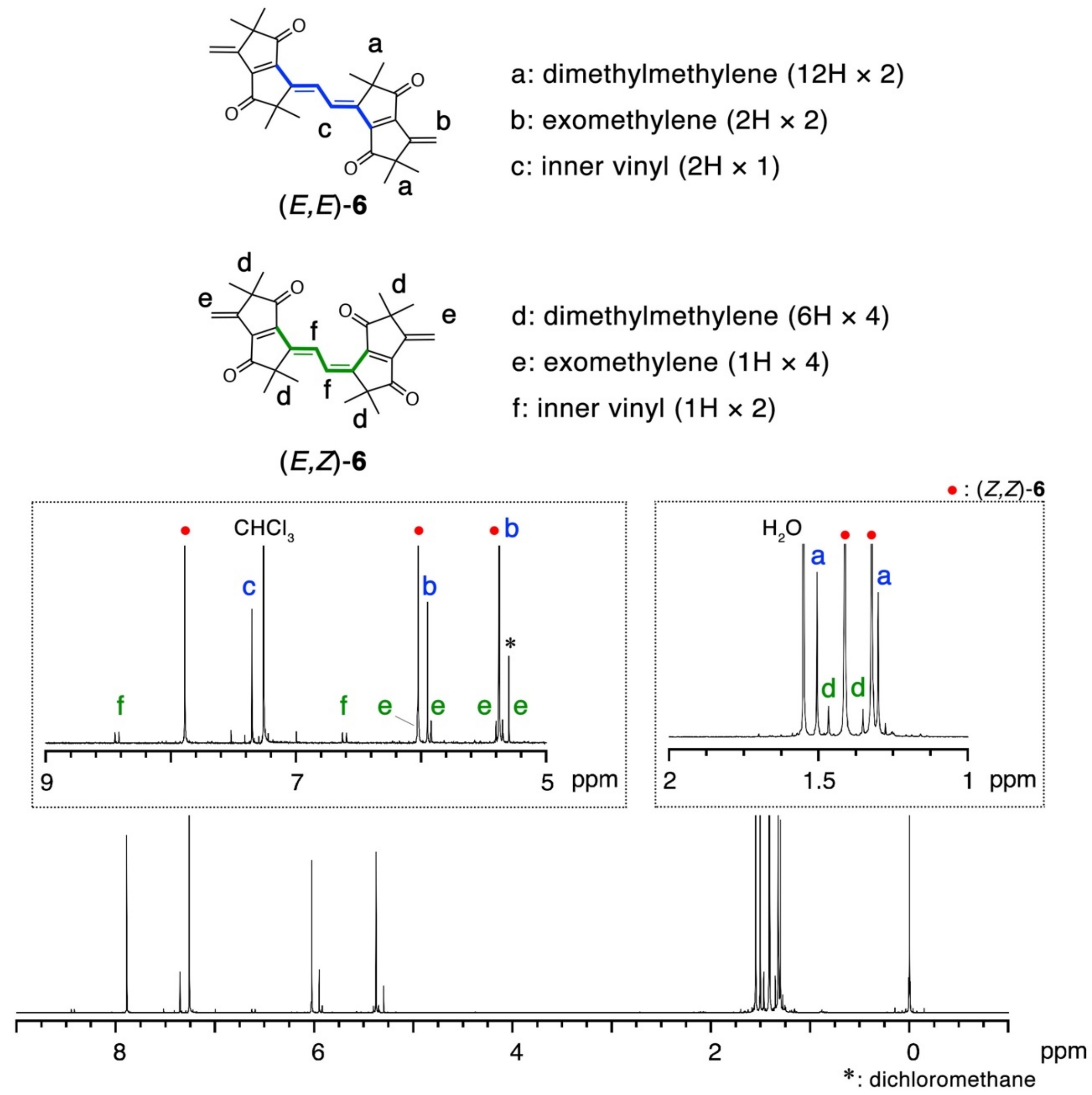

Figure S3. Assignment of (*E*,*E*)-**6** and (*E*,*Z*)-**6** in ^{1}H NMR spectrum of as-obtained **6**. Some peaks were overlapping with major peaks and estimated from the integration value.

Assignment of each isomer:

(*E*,*E*)-**6**: δ=7.35 (s, 2H, inner vinyl), 5.95 (s, 2H, terminal vinyl), 5.38 (s (overlapping), 2H, terminal vinyl), 1.51 (s, 12H, dimethylmethylene), 1.30 (s. 12H, dimethylmethylene).

(*E*,*Z*)-**6**: δ=8.43 (d, *J*=13.3 Hz, 1H, inner vinyl), 6.61 (d, *J*=13.3 Hz, 1H, inner vinyl), 6.03 (s, 1H, terminal vinyl), 5.92 (s, 1H, terminal vinyl), 5.40 (s, 1H, terminal vinyl), 5.35 (s, 1H, terminal vinyl), 1.47 (s, 6H, dimethylmethylene), 1.35 (s, 6H, dimethylmethylene), 1.31–1.33 (s × 2 (overlapping), 6H × 2, dimethylmethylene)

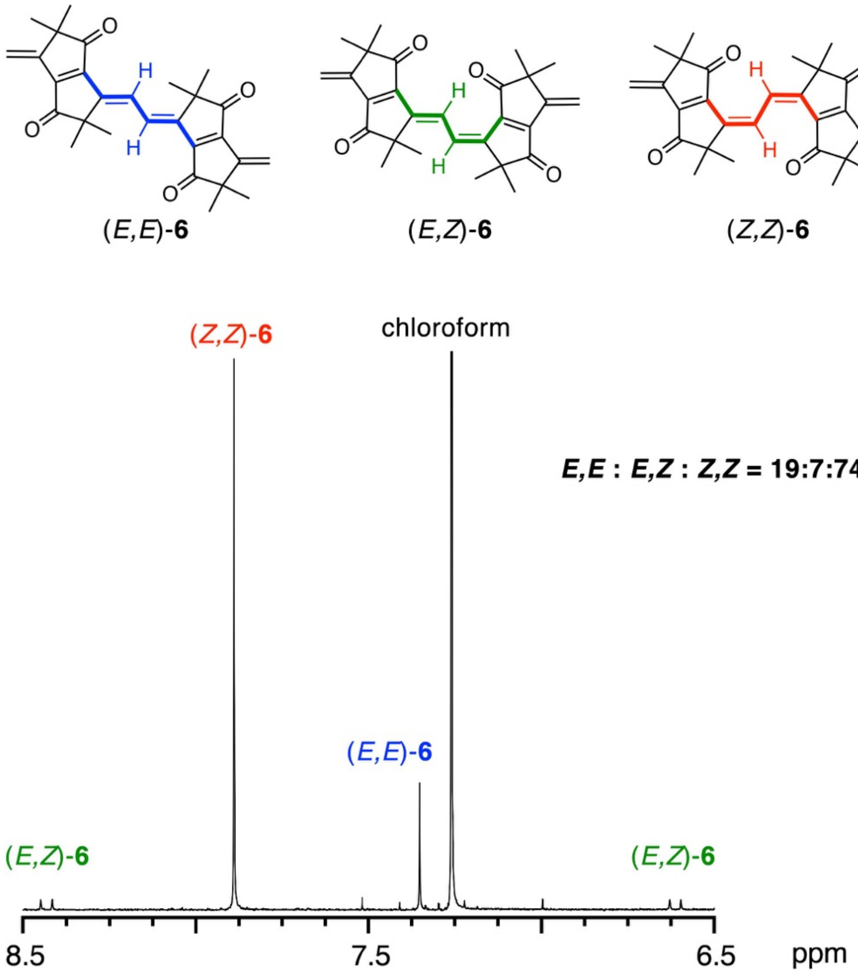

Figure S4. ^{1}H NMR spectrum of as-obtained **6**. The ratio of three isomers was calculated based on the integration value of inner vinyl protons.

2-5 Photo-rearrangement reaction of 6 into 7

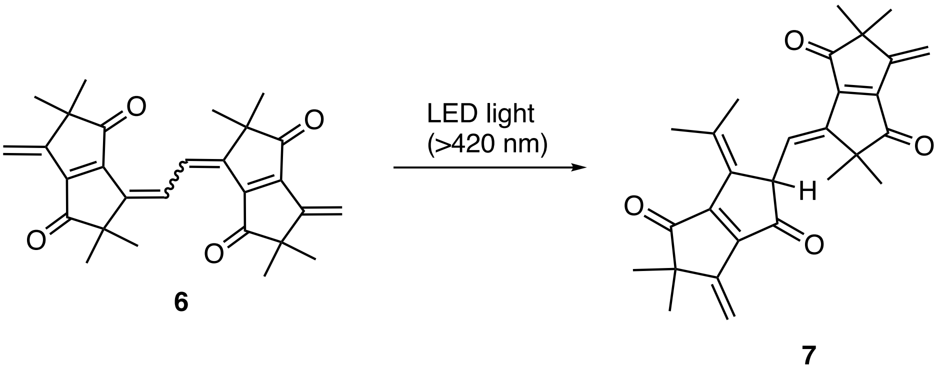

A degassed solution of a diastereomeric mixture of compound **6** (30.5 mg, 70 μmol) in 100 mL of chloroform in a 200 mL round-bottomed flask was exposed to 9W LED light (>420 nm; shorter wavelength region was cut-off using a filter; averaged distance from the light source is 10 cm) with stirring for 8 h at room temperature. The solvent was evaporated and the residue was chromatographed on a silica gel column (diameter 2.2 cm, height 10 cm, eluent: dichloromethane/hexane = 3:2). The main fraction (R_f=0.30) was collected, rinsed with hexane (3 mL), and filtered with suction to afford compound **7** (17.5 mg, 57% yield) as a pale yellow solid.

^{1}H NMR (400 MHz, $CDCl_3$, 298 K): δ=6.21 (d, J=10.6 Hz, 1H, inner vinyl), 5.92 (s, 1H, terminal vinyl), 5.87 (s, 1H, terminal vinyl), 5.33 (s, 1H, terminal vinyl), 5.26 (s, 1H, terminal vinyl); 4.47 (d, J=10.6 Hz, 1H, methine), 2.36 (s, 3H, methyl), 1.87(s, 3H, methyl), 1.64 (s, 3H, methyl), 1.51 (s, 3H, methyl), 1.30 (s, 3H, methyl), 1.27 (s, 3H, methyl), 1.26 (s, 3H, methyl), 1.25 (s, 3H, methyl); ^{13}C NMR (100 MHz, $CDCl_3$, 298 K): δ=206.4 (C=O), 205.9 (C=O), 204.5 (C=O), 198.5 (C=O), 161.4 (C=C), 157.8 (C=C), 157.7 (C=C), 155.4 (C=C), 145.9 (C=C), 145.5 (C=C), 142.9 (C=C), 140.6 (C=C), 127.3 (C=C), 126.7 (C=C), 112.4 (C=C), 111.3 (C=C), 58.4 (CH), 55.2 ($C(CH_3)_2$), 54.7 ($C(CH_3)_2$), 54.6 ($C(CH_3)_2$), 25.9 (CH_3), 24.6 (CH_3), 24.5 (CH_3), 24.25 (CH_3), 24.23 (CH_3), 23.9 (CH_3), 23.7 (CH_3), 23.3 (CH_3); IR (ATR, neat): 2965, 2927, 2869, 1705, 1651, 1626, 1460, 1383, 1309, 1207, 1142, 1113, 1049, 1024, 988 cm^{-1}; UV/Vis (dichloromethane): $\lambda_{max}(\varepsilon)$ = 251 (23000) 360 nm (12900 mol^{-1} L cm^{-1}); HRMS (APCI): *m/z* calcd for $C_{28}H_{29}O_4$: 429.2071 [M–H]$^-$; found: 429.2081; R_f=0.30 (hexane/ethyl acetate 10:1); m.p. 183 – 187 ºC (dec.).

III. Photo-isomerization of dodecahexaene 6

3-1 ^{1}H NMR monitoring of photo-isomerization of 6

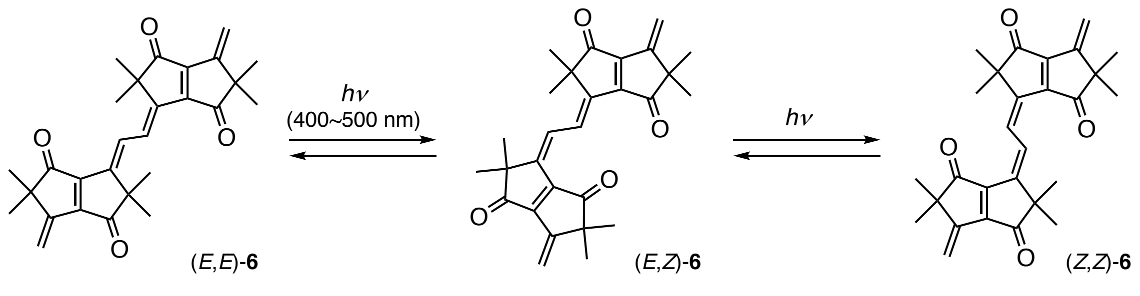

A 1.4×10^{-4} M solution of as-obtained **6** in $CDCl_3$ in NMR tube was placed under the room light (fluorescent light, 3000 lm, distance: 50 cm from the light source). ^{1}H NMR spectra were recorded after 0, 1, 5, and 10 h exposure.

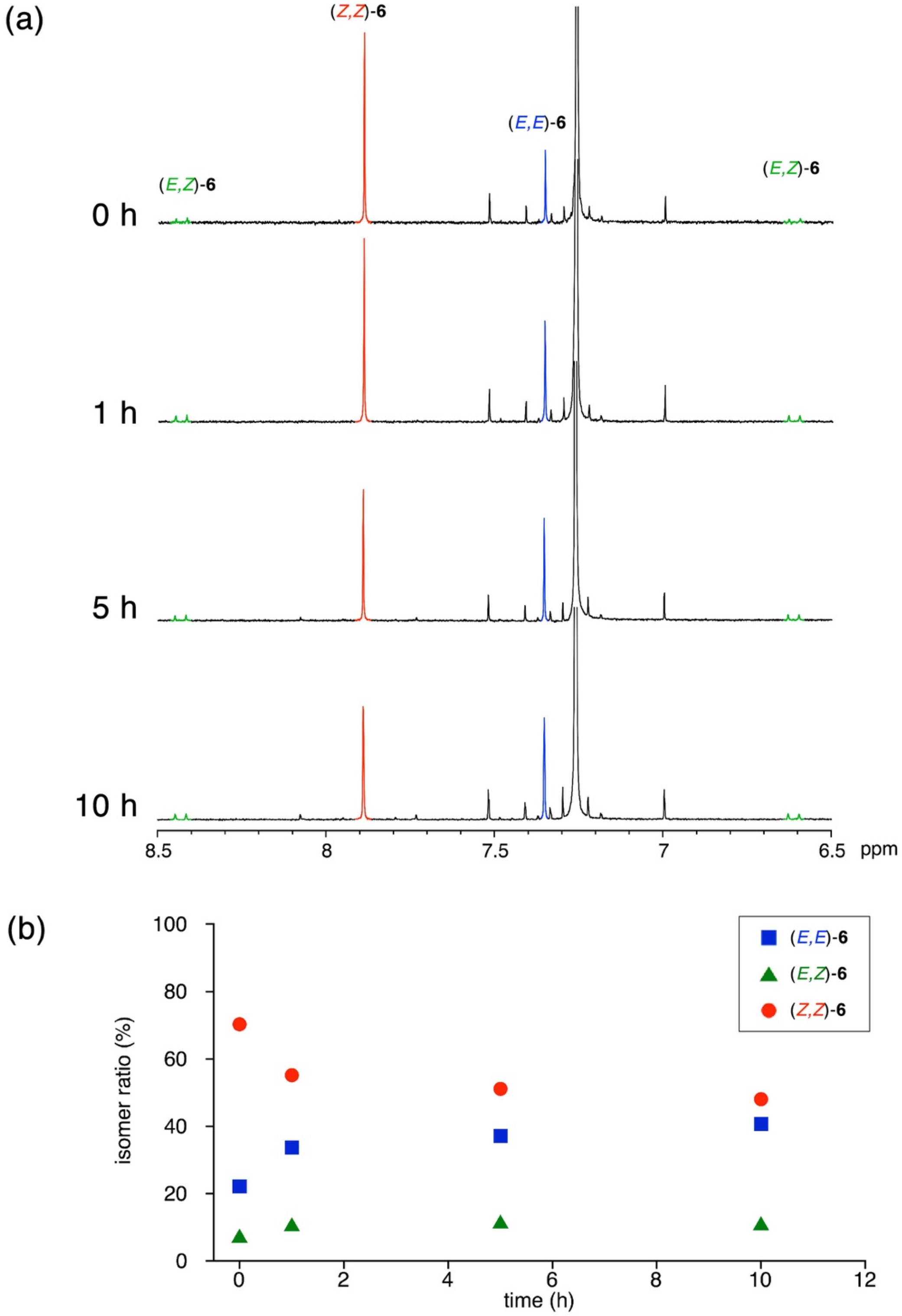

Figure S5. (a) Changes in the ^{1}H NMR spectra of $CDCl_3$ solution of compound **6** under room light. (b) A plot showing the relationship between ratio of each isomer and time of light exposure.

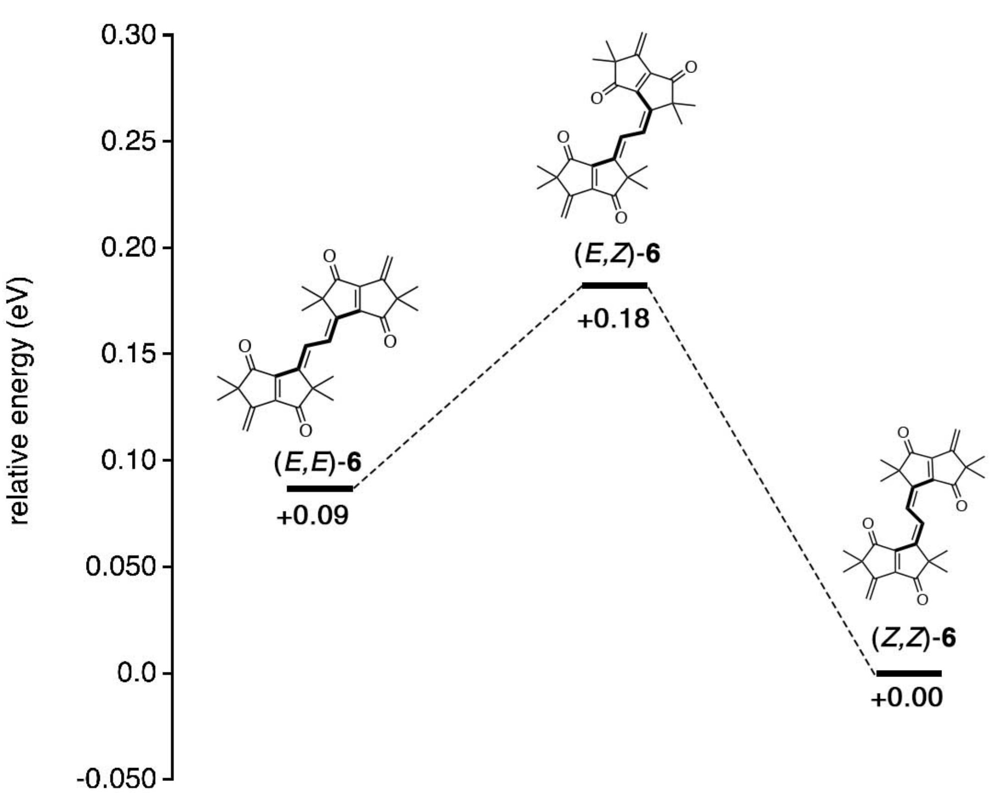

Figure S6. Comparison of heat of formation energy estimated by DFT calculations for three isomers of **6**. The calculations were performed at B3LYP/6-31G(d) level.

IV. Photo-rearrangement reaction of 6

4-1 Characterization of product 7

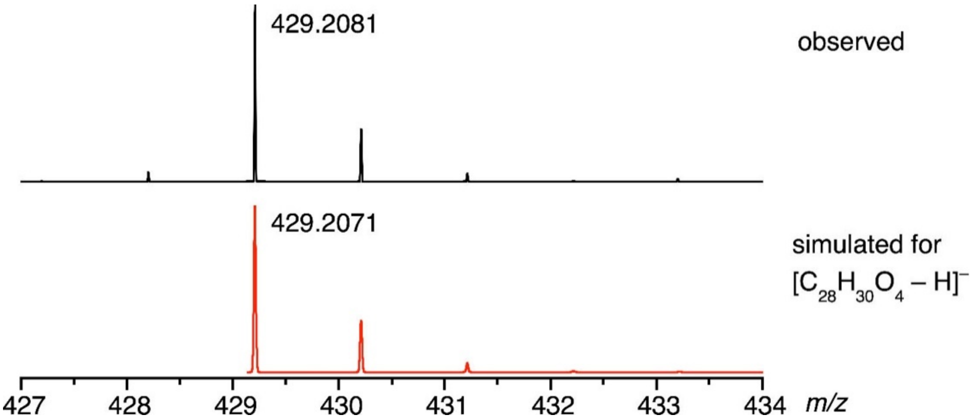

Figure S7. APCI-TOF mass spectrum (negative mode) of compound **7**. (black line: observed, red line: simulated)

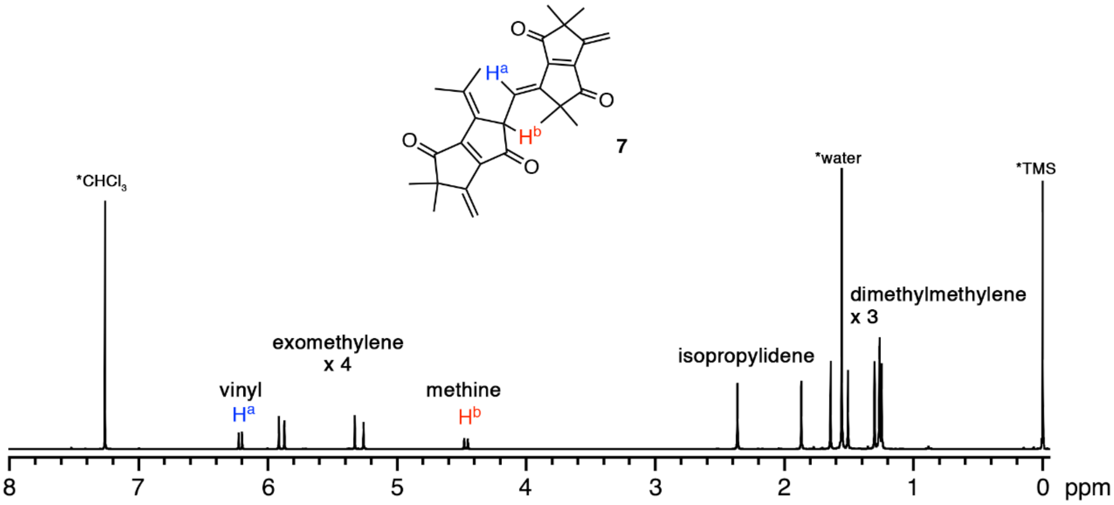

Figure S8. ^{1}H NMR spectrum of compound **7**.

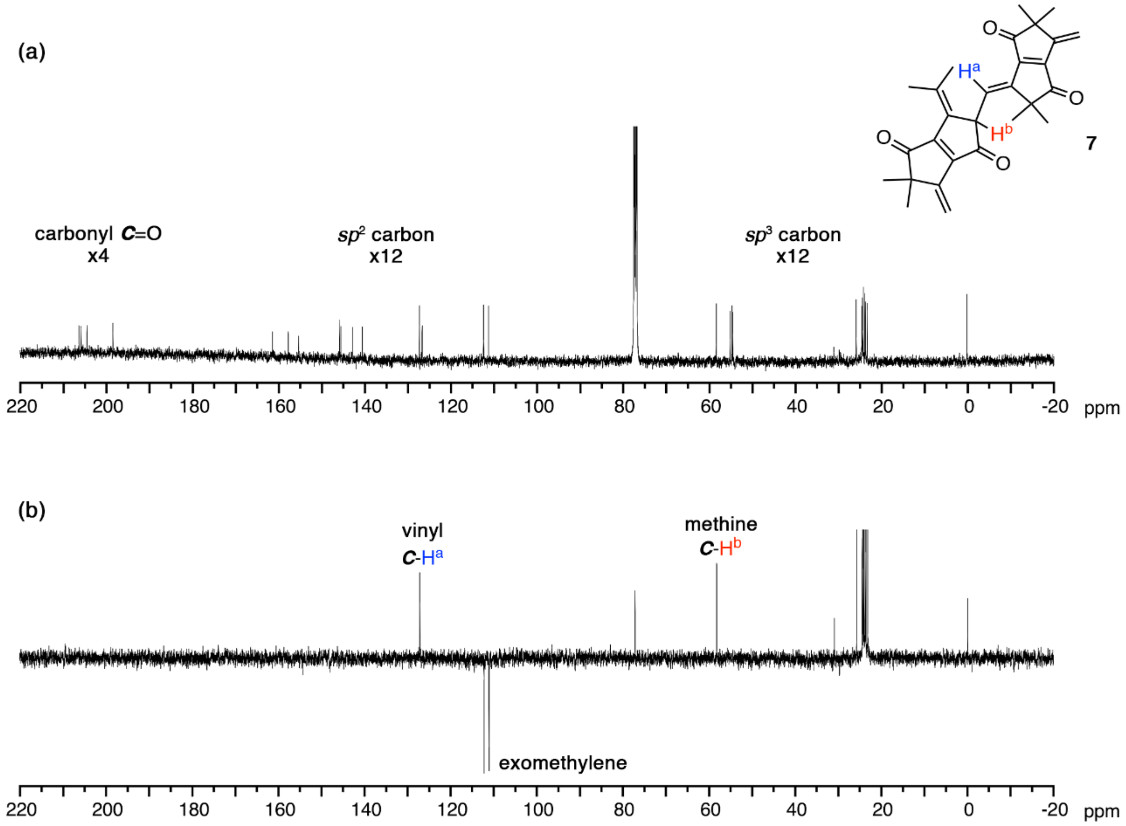

Figure S9. (a) $^{13}C\{^1H\}$ NMR and (b) DEPT135 spectra of compound **7**.

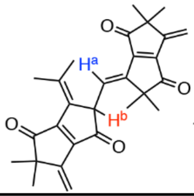

7

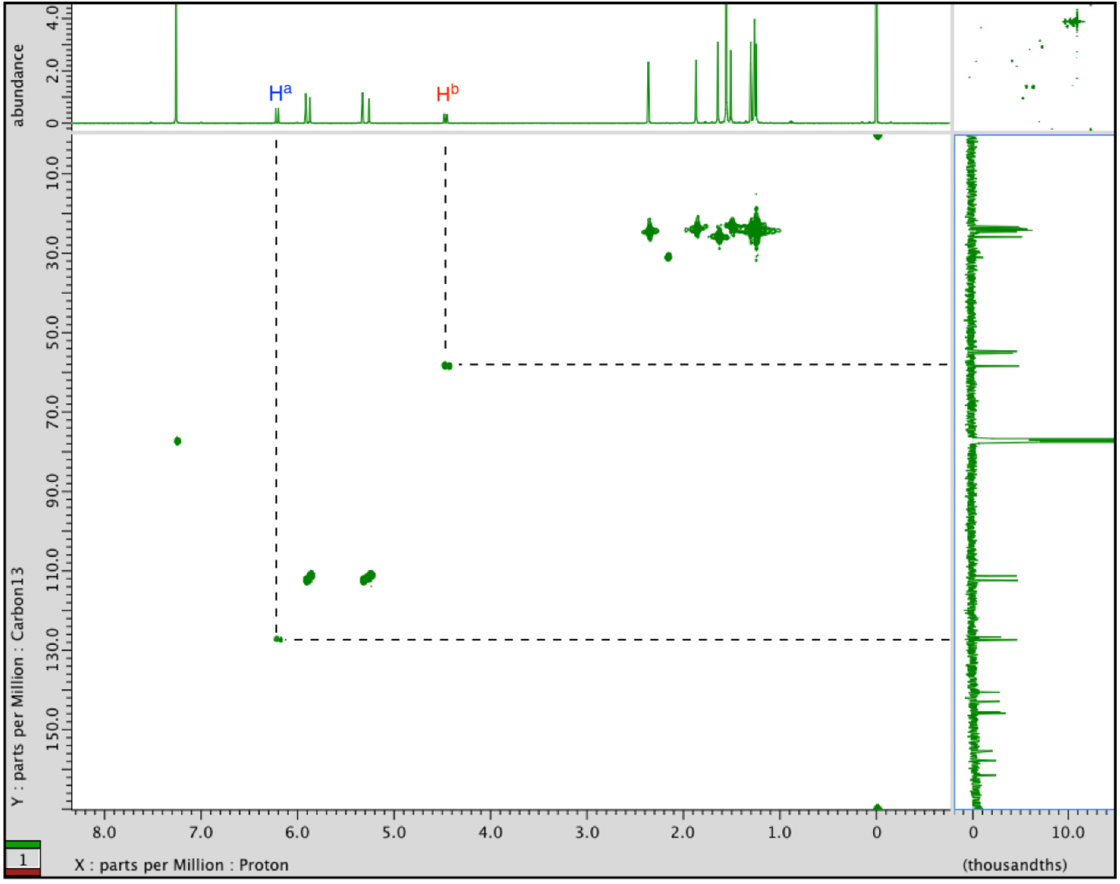

Figure S10. HMQC spectrum of compound **7**.

4-2 Proposed reaction mechanism

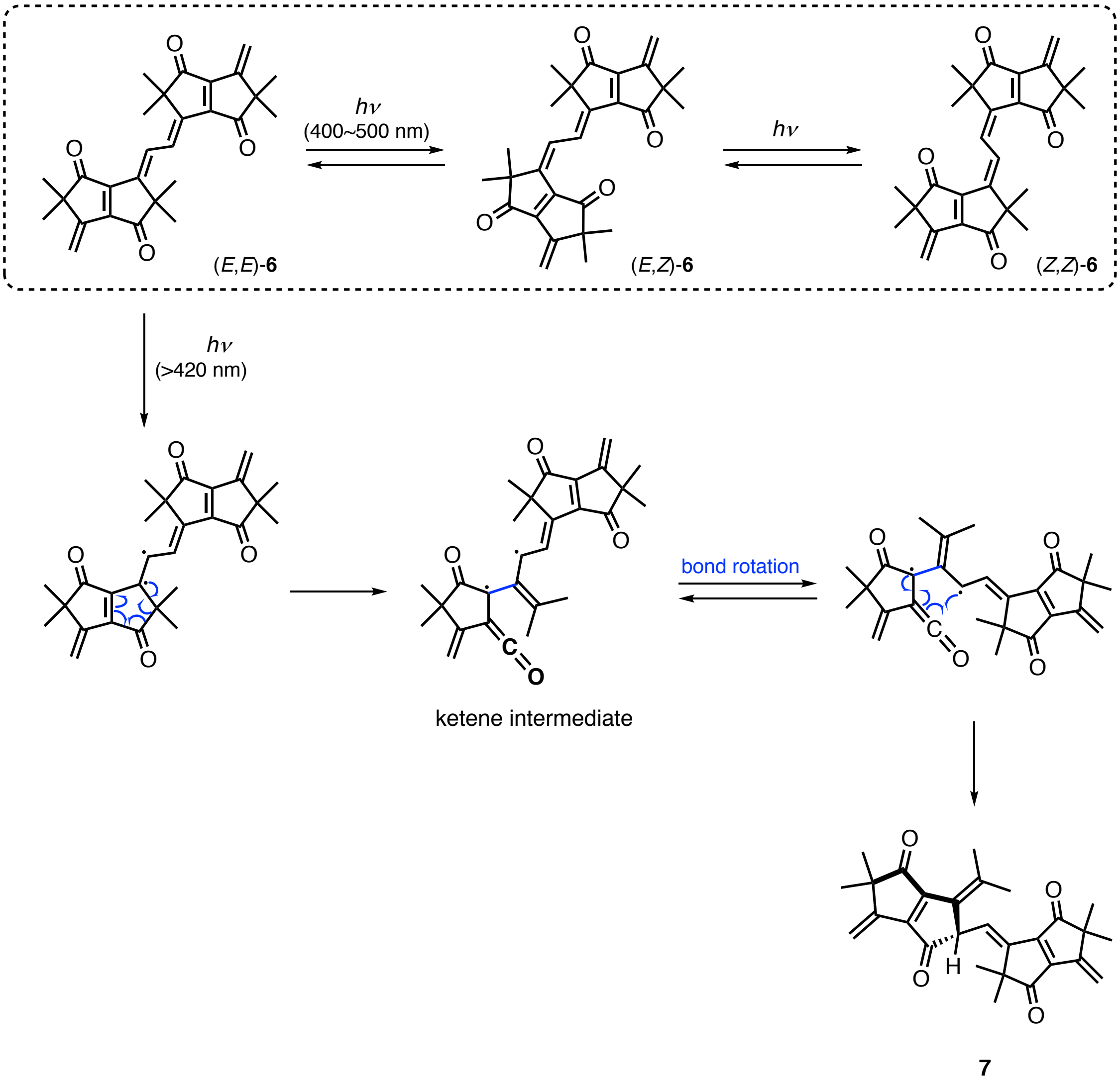

Scheme S1. Plausible reaction mechanism for photo-rearrangement reaction from **6** to **7**.

4-3 DFT calculations

Using the coordinates for crystal structures, geometries of **3**, (*Z*,*Z*)-**6** and **7** were optimized at the B3LYP/6-31G(d,p) level.

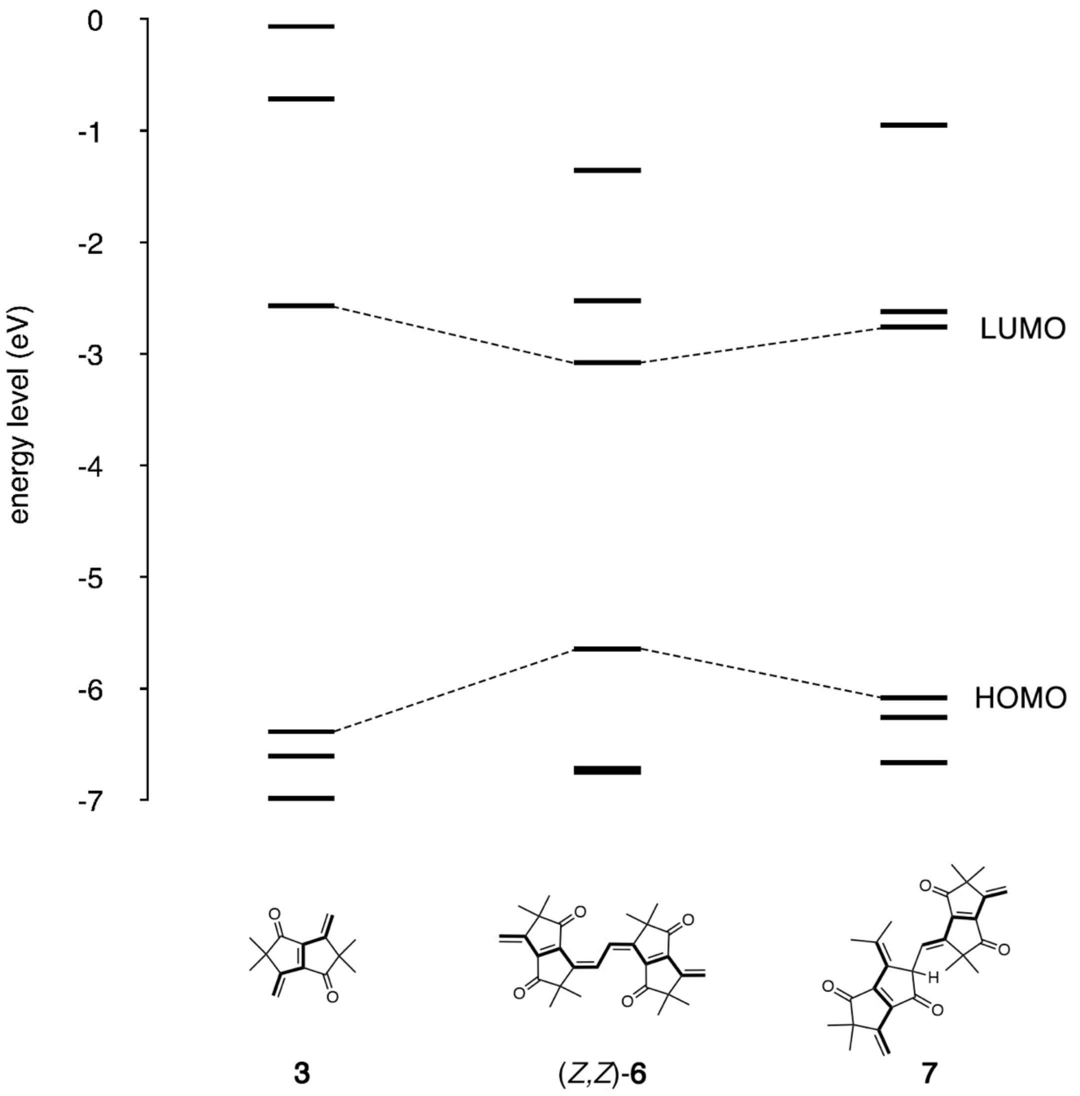

Figure S11. Energy levels of frontier orbitals for compounds **3**, (*Z*,*Z*)-**6** and **7** calculated at the B3LYP/6-31G(d,p) level.

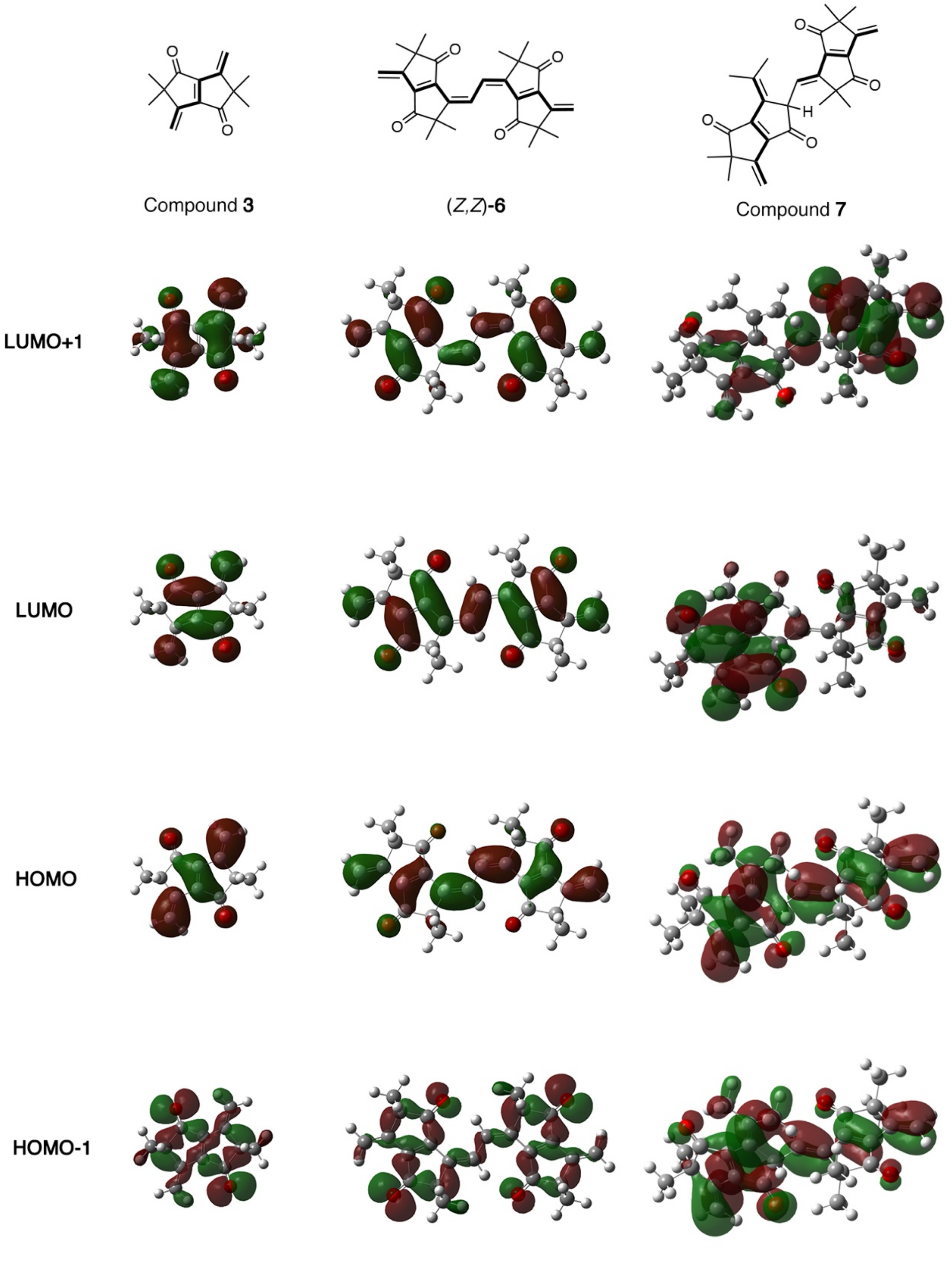

Figure S12. Orbital density diagrams of frontier orbitals for compounds **3**, (*Z*,*Z*)-**6** and **7** calculated at the B3LYP/6-31G(d,p) level.

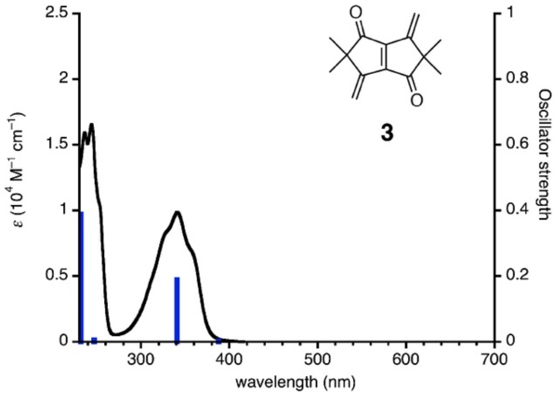

transition (1) (437.03 nm, f = 0.0000)
HOMO–1 --> LUMO (97%)

transition (2) (387.75 nm, f = 0.0020)
HOMO–2 --> LUMO (93%)
HOMO–1 --> LUMO+2 (2%)
HOMO --> LUMO (3%)

transition (3) (340.60 nm, f = 0.1883)
HOMO–2 --> LUMO (3%)
HOMO --> LUMO (91%)
HOMO --> LUMO+1 (5%)

transition (4) (272.20 nm, f = 0.0000)
HOMO–3 --> LUMO (94%)
HOMO --> LUMO+2 (4%)

transition (5) (259.64 nm, f = 0.0000)
HOMO–2 --> LUMO+2 (7%)
HOMO–1 --> LUMO+1 (89%)

transition (6) (246.75 nm, f = 0.0049)
HOMO–5 --> LUMO (3%)
HOMO–3 --> LUMO (3%)
HOMO–3 --> LUMO+1 (54%)
HOMO–1 --> LUMO+2 (35%)
HOMO --> LUMO+1 (2%)

transition (7) (231.66 nm, f = 0.3894)
HOMO–4 --> LUMO (5%)
HOMO --> LUMO (6%)
HOMO --> LUMO+1 (85%)

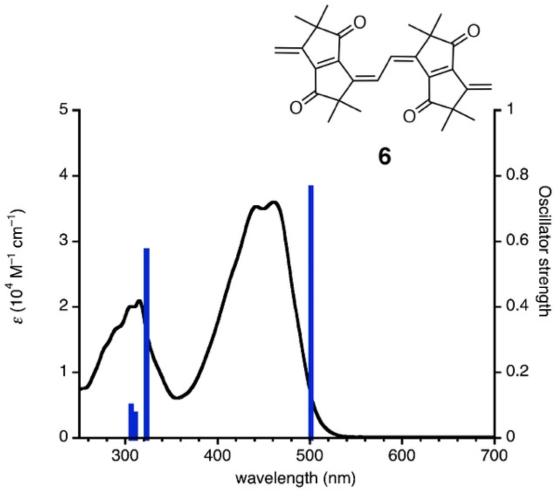

transition (1) (501.07 nm, f = 0.7642)
HOMO --> LUMO (98%)
HOMO --> LUMO+2 (2%)

transition (2) (463.68 nm, f = 0.0000)
HOMO–2 --> LUMO+1 (17%)
HOMO–1 --> LUMO (80%)

transition (3) (460.10 nm, f = 0.0000)
HOMO–3 --> LUMO (5%)
HOMO --> LUMO+1 (93%)

transition (4) (459.38 nm, f = 0.0000)
HOMO–2 --> LUMO (77%)
HOMO–1 --> LUMO+1 (20%)

transition (5) (398.26 nm, f = 0.0003)
HOMO–5 --> LUMO+1 (22%)
HOMO–4 --> LUMO (73%)

transition (6) (397.72 nm, f = 0.0000)
HOMO–5 --> LUMO (74%)
HOMO–4 --> LUMO+1 (23%)

transition (9) (344.15 nm, f = 0.0000)
HOMO–3 --> LUMO (89%)
HOMO --> LUMO+1 (4%)
HOMO --> LUMO+3 (4%)

transition (10) (322.96 nm, f = 0.5716)
HOMO–6 --> LUMO (18%)
HOMO --> LUMO (3%)
HOMO --> LUMO+2 (78%)

transition (13) (310.71 nm, f = 0.0736)
HOMO–6 --> LUMO (2%)
HOMO–3 --> LUMO+1 (93%)

transition (14) (310.71 nm, f = 0.0736)
HOMO–6 --> LUMO (2%)
HOMO–3 --> LUMO+1 (93%)

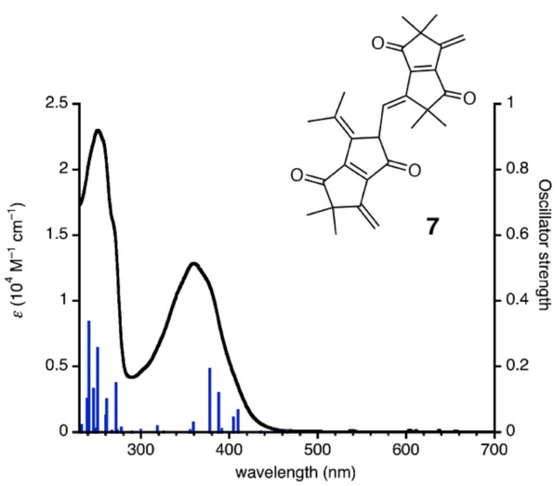

transition (1) (465.61 nm, f = 0.0050)
HOMO–5 --> LUMO (3%)
HOMO–3 --> LUMO (14%)
HOMO–1 --> LUMO (28%)
HOMO --> LUMO (50%)

transition (2) (435.67 nm, f = 0.0006)
HOMO–2 --> LUMO (9%)
HOMO–2 --> LUMO+1 (87%)

transition (3) (409.65 nm, f = 0.0656)
HOMO–5 --> LUMO (3%)
HOMO–3 --> LUMO (35%)
HOMO–3 --> LUMO+1 (2%)
HOMO–1 --> LUMO (9%)
HOMO–1 --> LUMO+1 (3%)
HOMO --> LUMO (31%)
HOMO --> LUMO+1 (11%)

transition (4) (404.65 nm, f = 0.0430)
HOMO–5 --> LUMO (3%)
HOMO–3 --> LUMO (19%)
HOMO–1 --> LUMO+1 (16%)
HOMO --> LUMO+1 (54%)

transition (5) (391.37 nm, f = 0.0088)
HOMO–4 --> LUMO (7%)
HOMO–4 --> LUMO+1 (79%)
HOMO–3 --> LUMO+1 (4%)

transition (6) (387.91 nm, f = 0.1180)
HOMO–5 --> LUMO (19%)
HOMO–4 --> LUMO (2%)
HOMO–3 --> LUMO (8%)
HOMO–1 --> LUMO (35%)
HOMO–1 --> LUMO+1 (6%)
HOMO --> LUMO (15%)
HOMO --> LUMO+1 (7%)

transition (7) (377.80 nm, f = 0.1922)
HOMO–4 --> LUMO+1 (2%)
HOMO–1 --> LUMO (2%)
HOMO–1 --> LUMO+1 (69%)
HOMO -->LUMO+1 (20%)

transition (8) (359.17nm, f = 0.0287)
HOMO–7 --> LUMO (3%)
HOMO–5 --> LUMO (37%)
HOMO–3 --> LUMO (9%)
HOMO–2 --> LUMO (28%)
HOMO–2 --> LUMO+1 (30%)
HOMO–1 --> LUMO (16%)

transition (9) (355.44 nm, f = 0.0044)
HOMO–5 --> LUMO (18%)
HOMO–3 --> LUMO (5%)
HOMO–2 --> LUMO (61%)
HOMO–2 --> LUMO+1 (6%)
HOMO–1 --> LUMO (4%)

transition (10) (325.55 nm, f = 0.0004)
HOMO–5 --> LUMO (3%)
HOMO–4 --> LUMO (84%)
HOMO–4 --> LUMO+1 (7%)

Figure S13. TD-DFT calculated (at the B3LYP/6-31G(d,p) level) absorption bands for compounds **3**, (*Z*,*Z*)-**6** and **7**.

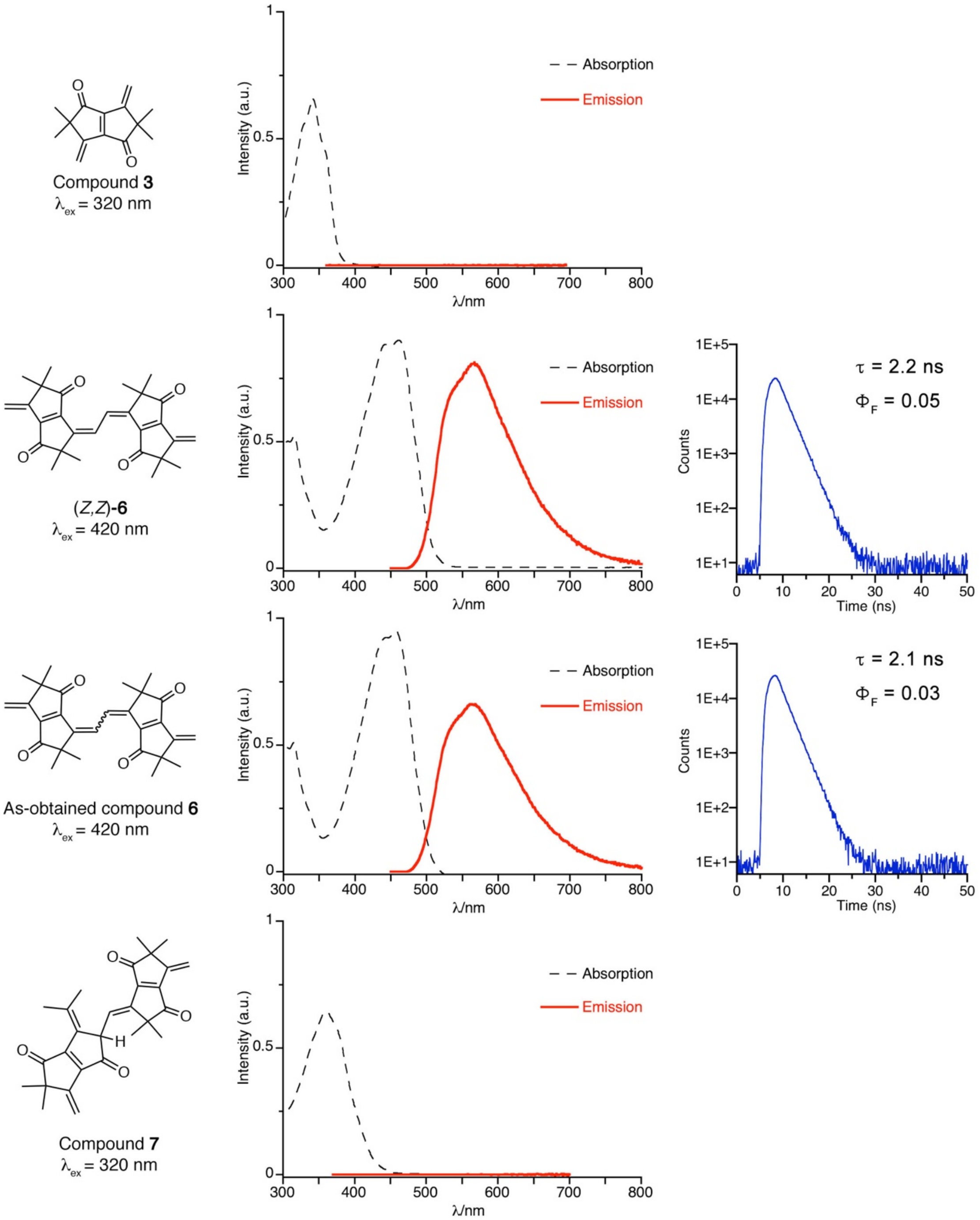

Figure S14. (Left) Fluorescence (red, solid line) and absorption (black, dashed line) spectra of compounds **3**, (*Z,Z*)-**6**, as-obtained *E/Z* mixture of **6**, and **7** in CH_2Cl_2. (Right) Fluorescence decay (blue line) of (*Z,Z*)-**6** and as-obtained *E/Z* mixture of **6**.

4-4 Estimation of dipole-dipole coupling

Förster-type excitonic interaction is approximated by two dipoles interacting each other through dipole-dipole interaction, U,

$$U = \frac{1}{4\pi\epsilon_0}\frac{1}{r^3}[\boldsymbol{p}_1 \cdot \boldsymbol{p}_2 - 3(\boldsymbol{p}_1 \cdot \boldsymbol{r})(\boldsymbol{p}_1 \cdot \boldsymbol{r})],$$

where ϵ_0 is the permittivity of vacuum; r and $\boldsymbol{r}$ are the distance and the vector between two chromophores, respectively; $\boldsymbol{p_1}$ and $\boldsymbol{p_2}$ are the dipole vector of the dipole 1 and 2, respectively. The position of the dipoles in the compound **3** are obtained from the crystalline structure. The parameters used in the simulation are listed in the Table S1.

Table S1. The parameters for the dipole-dipole interaction calculation

	$\boldsymbol{r}$ (Å)	Dipole 1 (Debye)	Dipole 2 (Debye)
X	6.3677	-4.4651	3.6915
Y	-0.1606	-1.3797	-3.9157
Z	-0.0346	2.7503	0.6672

4-5. Analysis of absorption spectra based on Holstein model with multi-particle basis set

4-5-1. Description of the Holstein model calculation

Here, we describe a model based on the exciton theory with a Holstein-type Hamiltonian[6–8] for simulating the spectral features of absorption bands observed in the UV-Vis spectra. The model consists of two chromophores. The one-exciton Hamiltonian in the electronically excited state, H, is given below in the manner of the conventional Holstein-type model. We assume that the electronic transition is coupled to only one intramolecular vibrational mode of a frequency ω_ν and the potential curves with respect to this mode in the ground and electronically excited states are all harmonic:

$$H = H_\mathrm{e} + H_\mathrm{ph} + H_\mathrm{e-ph}$$

$$H_\mathrm{e} = \sum_{i=1,2} E_0 a_i^+ a_i + J(a_2^+ a_1 + a_1^+ a_2)$$

$$H_\mathrm{ph} = \sum_{i=1,2} \hbar\omega_\nu b_i^+ b_i$$

$$H_\mathrm{e-ph} = \sum_{i=1,2} \hbar\omega_\nu g a_i^+ a_i (b_i^+ + b_i),$$

where, E_0 is the energy of a dipole-allowed electronically excited state; a_i^+ (a_i) is the creation (annihilation) operator for an excited state localized at a molecule i, b_i^+ (b_i) is the creation (annihilation) operator for a coupled phonon at the same molecule; J is the intermolecular electronic coupling between the two chromophores; and g is the electron-phonon coupling constant.

In the case of materials composed of neutral organic molecules, electronic excitations result in the formation of Frenkel excitonic polarons: a Frenkel exciton surrounded by vibrationally (but not electronically) excited molecules. In this work, we represent the Hamiltonian with a localized basis set under the two-particle approximation (TPA): a single vibronic excitation plus a vibronic/vibrational pair excitation. We denote the wave function of a molecule i as $\phi_i^{e(\nu)}$, where the molecule is in the electronic state e ($e = \mathrm{gr}, \mathrm{ex}$ denotes the electronic ground state, and the excited state, respectively) with vibrational quanta ν. The localized one- and two-particle states of electronically excited state in the two chromophores ($i, j = 1$ or $2,\ i \neq j$) are

$$|\mathrm{ex}; i\ \tilde{\nu}\rangle = \left|\phi_i^{\mathrm{ex}(\tilde{\nu})} \phi_j^{\mathrm{gr}(0)}\right\rangle$$

and

$$|\mathrm{ex}; i\,\tilde{\nu}, \nu\rangle = \left|\phi_i^{\mathrm{ex}(\tilde{\nu})}\phi_j^{\mathrm{gr}(\nu)}\right\rangle$$

respectively. Here, $\tilde{\nu}$ is the vibrational quanta of a displaced harmonic vibrational mode in the electronically excited state. In a one-particle state, a molecule at a site i is vibronically excited, while all the other molecules are in the vibrationless ground state. In a two-particle state, in addition to vibronic excitation of a molecule at i, a molecule at j is vibrationally excited in the electronic ground state.

The kth eigenstate of the exciton can be expanded by these basis sets as

$$|\Psi_k^{\mathrm{ex}}\rangle = \sum_{i,\tilde{\nu}} c_{i,\tilde{\nu}}^k |\mathrm{ex}; i\,\tilde{\nu}\rangle + \sum_{i,\tilde{\nu},\nu} c_{i,\tilde{\nu},\nu}^k |\mathrm{ex}; i\,\tilde{\nu}, \nu\rangle$$

where $c_{i,\tilde{\nu}}^j$, and $c_{i,\tilde{\nu},\nu}^j$ are coefficients for one- and two- particle states, respectively. The coefficients are evaluated numerically by diagonalization of the Hamiltonian with the basis sets of one- and two-particle states in the momentum space.

Electronic absorption spectra of holes $A(E)$ are calculated with

$$A(E) \propto \sum_k \left|\left\langle\Psi_k^{\mathrm{ex}}\middle|\hat{\mu}\middle|\phi_1^{\mathrm{gr}(0)}\phi_2^{\mathrm{gr}(0)}\right\rangle\right|^2 \times \Gamma(E - E_k)$$

where Ψ_k^{ex} is the kth final electronic states; E_k is the eigenenergies of $|\Psi_k^{\mathrm{ex}}\rangle$; μ is the dipole moment operator, and $\Gamma(E)$ is the line-shape function.

In the numerical evaluations of absorption spectra as a function of intermolecular electronic coupling strength, we fixed the maximum vibrational quanta of ν and $\tilde{\nu}$ to be 5 for describing phonon-dressed excited states.

4-5-2. Exciton coupling between the chromophores estimated form UV-Vis spectra

Firstly, we determined intramolecular parameters from comparison of a simulated spectrum to the experimentally observed UV-Vis spectrum of **3** which represent an isolated chromophore of the triene. The frequency of the vibrational mode of interest ω_v was set to be $\hbar\omega_v$ = 1452 cm^{-1} obtained from the vibronic progression. The electron-phonon coupling constant was estimated to be 1.24. The line shape of each transition was assumed to be Gaussian function, $\Gamma(E) = \exp\left(-\frac{E^2}{\gamma^2}\right)$, with γ = 988 cm^{-1}. E_0 was set to be 27826 cm^{-1}. With those parameters, the experimental UV-Vis spectrum was reproduced (Figure S15(a)). The clear vibronic progressions in the spectrum indicate that the eigenstates with different vibrational quanta are discretely separated.

The exciton coupling between chromophores mixes the vibronic eigenstates, resulting in modification in a vibronic line shape such as the ratio between absorbance of 0-0 and 0-1 vibronic transitions. Besides the spectrum of **7** shows additional broad band around 24200 cm^{-1} due to breaking symmetry of the molecular orbitals of the chromophore, we can distinguish that the ratio of the intensity of the 0-0 transition (~26350 cm^{-1}) and the 0-1 transition (~27800 cm^{-1}) was significantly modified when compared to that of **3**. The spectral shape was reasonably reproduced by considering inter-chromophore excitonic coupling J = –540 cm^{-1} and E_0 = 26616 cm^{-1} (Figure S15(b)).

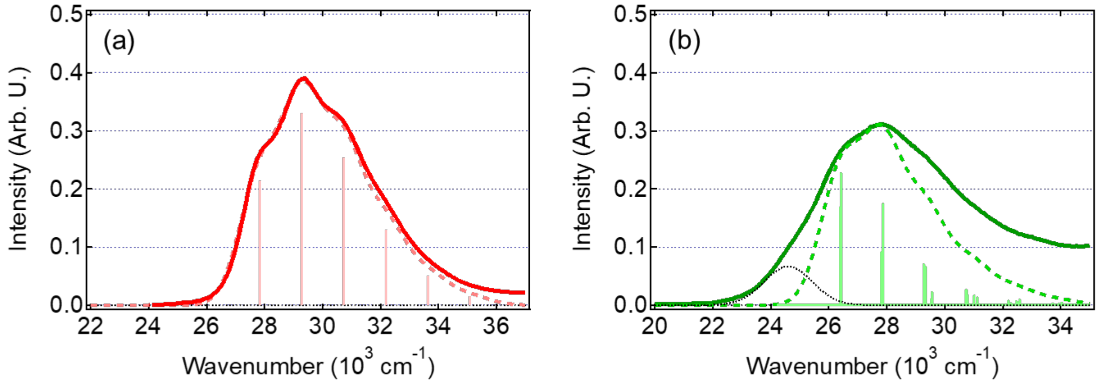

Figure S15. Comparison of the spectral calculations based on the Holstein model described in the section 4-5-1 (dashed lines and bars) and experimentally observed UV-Vis spectra (solid lines). The bars indicate calculated absorption. The dashed lines are Gaussian convoluted spectra of the calculations: (a) Compound **3**, and (b) Compound **7**. The black dotted line indicate absorption from lower-lying energy absorption activated due to symmetry breaking.

V. X-ray Crystallographic Analysis of 5

Single crystal X-ray diffraction data for **3**

$C_{14}H_{16}O_2$, $M = 216.27$, crystal size: 0.25 × 0.20 × 0.09 mm^3, Monoclinic, space group $P2_1/c$, $a = 8.8117(5)$ Å, $b = 5.8923(3)$ Å, $c = 11.6496(7)$ Å, $\beta = 101.722(5)$°, $V = 592.25(6)$ Å^3, $Z = 2$, $T = 123(2)$ K, $\mu = 0.080$ mm^{-1}, $D_{\text{calc}} = 1.213$ g/cm^3, $3.862° \leq \theta \leq 26.492°$, 1086 unique reflections out of 1219 with $I > 2\sigma(I)$, GOF = 1.028, $R_1 = 0.0360$, $wR_2 = 0.0933$. CCDC deposit number: 1954077.

Single crystal X-ray diffraction data for **5**

$C_{28}H_{34}O_4$, $M = 434.55$, crystal size: 0.32 × 0.29 × 0.06 mm^3, Monoclinic, space group $P2_1/c$, $a = 8.6894(4)$ Å, $b = 5.8144(3)$ Å, $c = 23.4264(12)$ Å, $\beta = 99.837(5)$°, $V = 1166.19(10)$ Å^3, $Z = 2$, $T = 123(2)$ K, $\mu = 0.081$ mm^{-1}, $D_{\text{calc}} = 1.238$ g/cm^3, $2.647° \leq \theta \leq 27.493°$, 2397 unique reflections out of 2775 with $I > 2\sigma(I)$, GOF = 1.078, $R_1 = 0.0760$, $wR_2 = 0.2395$. CCDC deposit number: 1954078.

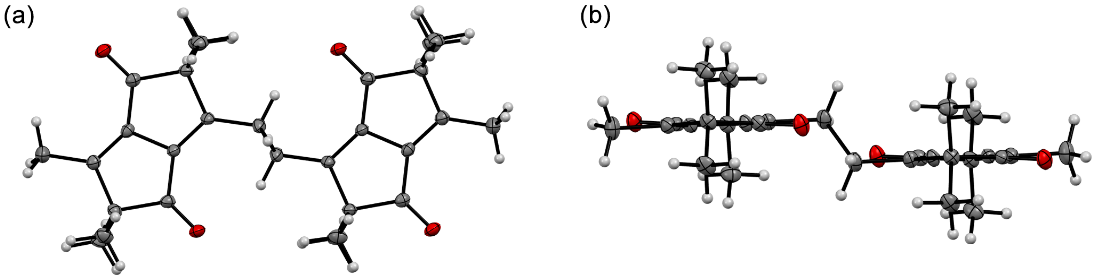

Figure S16. ORTEP drawing of the crystal structure of compound **5** (a) top and (b) side. Thermal ellipsoids are drawn at the 50% probability level.

Single crystal X-ray diffraction data for (*Z,Z*)-**6**

$C_{28}H_{30}O_4$, $M = 430.52$, crystal size: 0.20 × 0.20 × 0.03 mm^3, Monoclinic, space group $P2_1/c$, $a = 8.7961(6)$ Å, $b = 5.8385(4)$ Å, $c = 22.8947(14)$ Å, $\beta = 99.317(6)$°, $V = 1160.27(13)$ Å^3, $Z = 2$, $T = 123(2)$ K, $\mu = 0.081$ mm^{-1}, $D_{\text{calc}} = 1.232$ g/cm^3, $2.647° \leq \theta \leq 25.496°$, 1718 unique reflections out of 2191 with $I > 2\sigma(I)$, GOF = 1.122, $R_1 = 0.0814$, $wR_2 = 0.2250$. CCDC deposit number: 1954079.

Single crystal X-ray diffraction data for **7**

$C_{28}H_{30}O_4$, $M = 430.52$, crystal size: $0.68 \times 0.20 \times 0.11$ mm^3, Monoclinic, space group $P2_1/c$, $a = 12.6447(4)$ Å, $b = 17.9325(5)$ Å, $c = 10.8014(3)$ Å, $\beta = 103.228(3)$°, $V = 2384.24(12)$ Å^3, $Z = 4$, $T = 123(2)$ K, $\mu = 0.079$ mm^{-1}, $D_{calc} = 1.199$ g/cm^3, $2.245° \leq \theta \leq 26.493°$, 4438 unique reflections out of 4934 with $I > 2\sigma(I)$, GOF = 1.052, $R_1 = 0.0391$, $wR_2 = 0.1036$. CCDC deposit number: 1954080.

VI. CD Spectroscopy of 7

6-1 Optical resolution of 7

Enantiomers of **7** were separated on a CHIRAL ART Cellulose-SB (5 μm) column (length 250 mm, diameter 4.6 mm) using hexane/2-propanol (v/v= 98/2) as an eluent (flow rate: 0.5 mL/min) at room temperature. Analytical samples for CD spectroscopy were obtained by repeated separation using analytical HPLC.

6-2 TD-DFT calculation

TD-DFT calculations were performed using coordinates of crystal structures both for *S*-**7** and *R*-**7** at the B3LYP/6-31G(d,p) level.

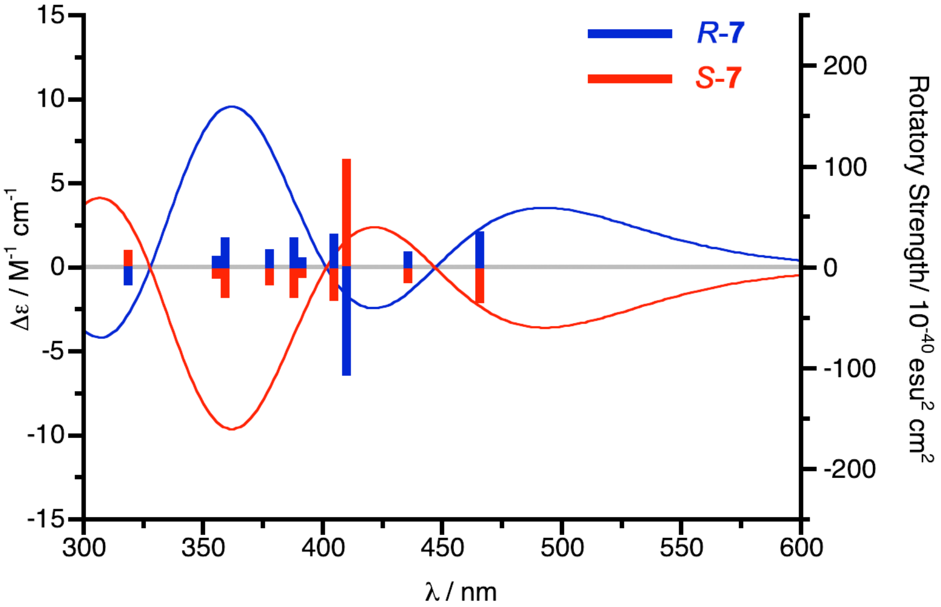

Figure S17. TD-DFT calculation CD spectra of compound *R*-**7** (blue) and *S*-**7** (red). The simulated spectra were drawn with the Half-Width at Half-Height of 2500 cm^{-1}. Bars show the calculated rotatory strength of *R*-**7** (blue) and *S*-**7** (red).

VII. NMR Spectra

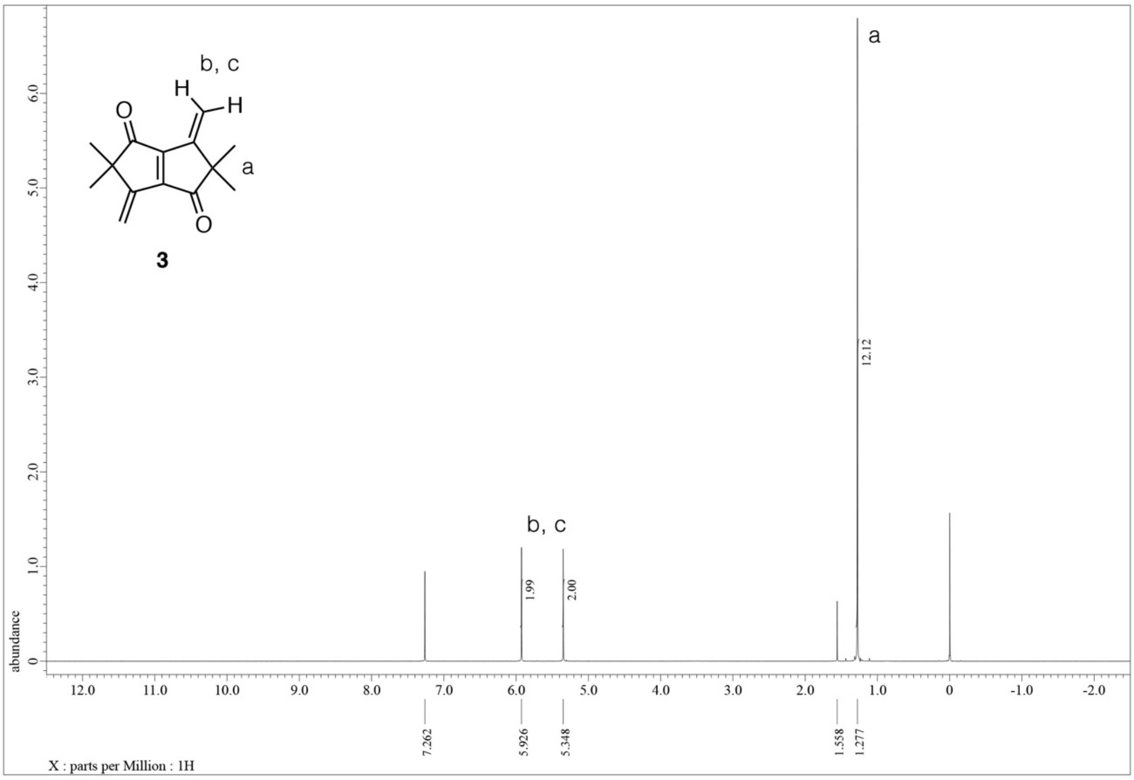

Figure S18. ^{1}H NMR spectrum of compound **3** in $CDCl_3$.

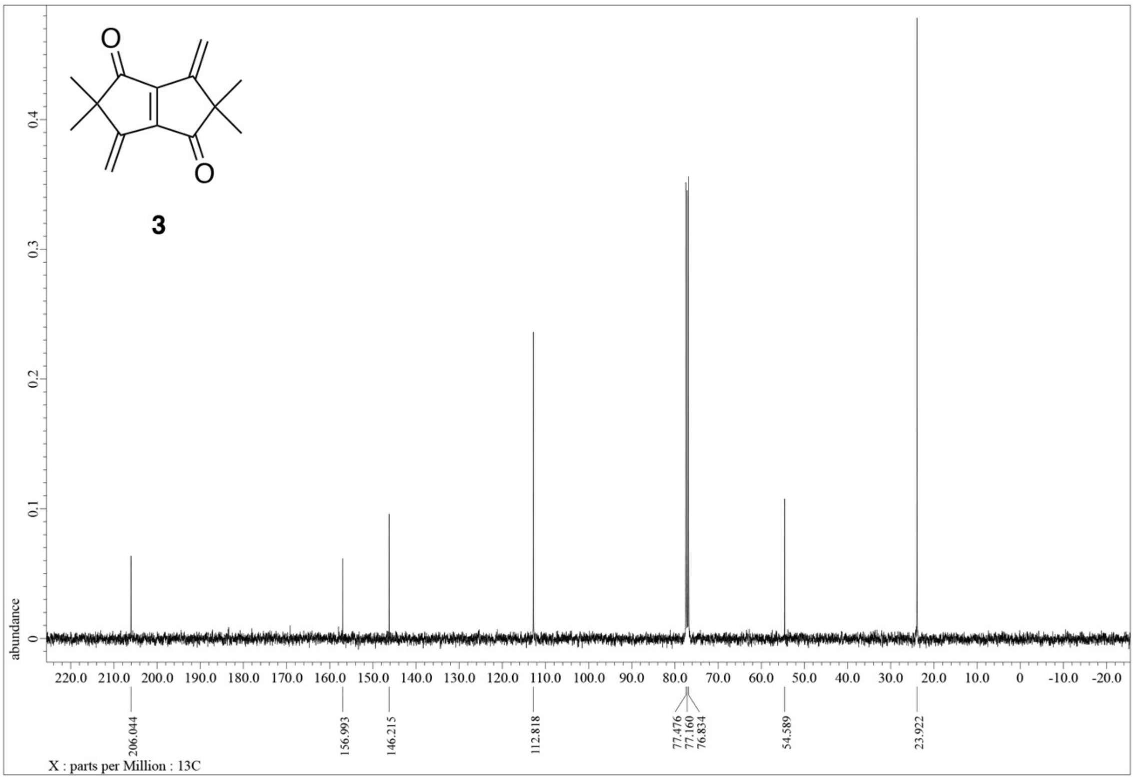

Figure S19. $^{13}C\{^1H\}$ NMR spectrum of compound **3** in $CDCl_3$.

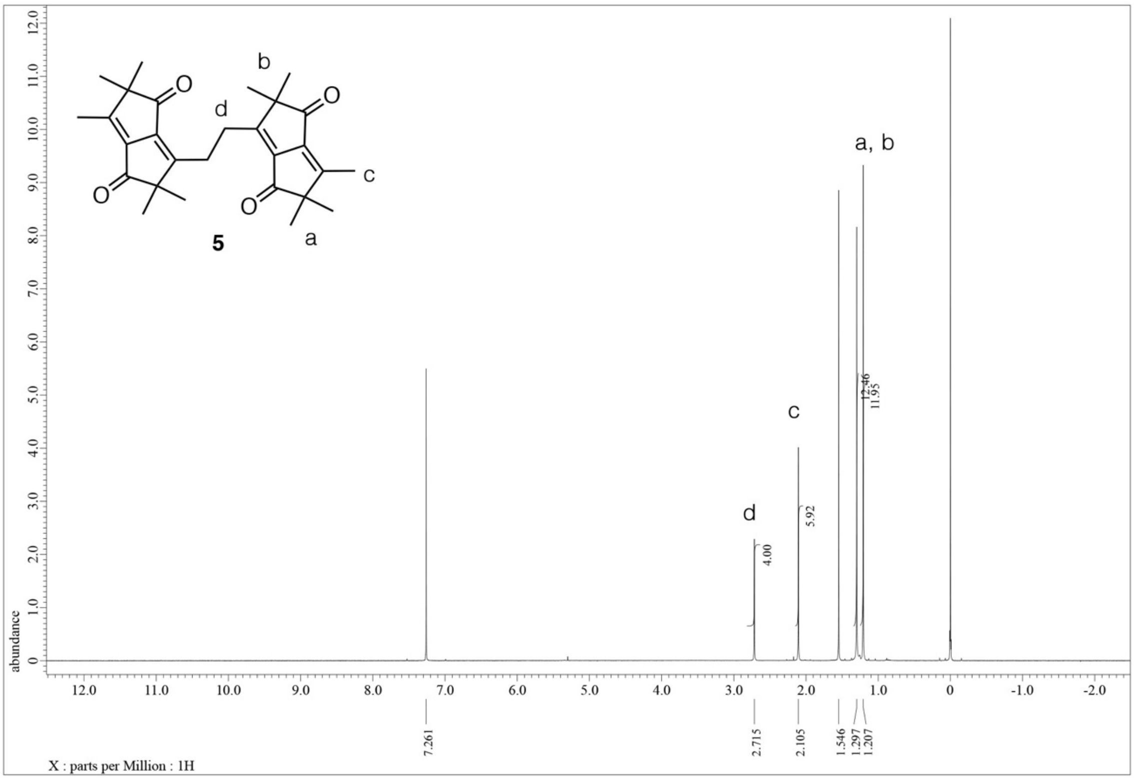

Figure S20. ^{1}H NMR spectrum of compound **5** in CDCl$_3$.

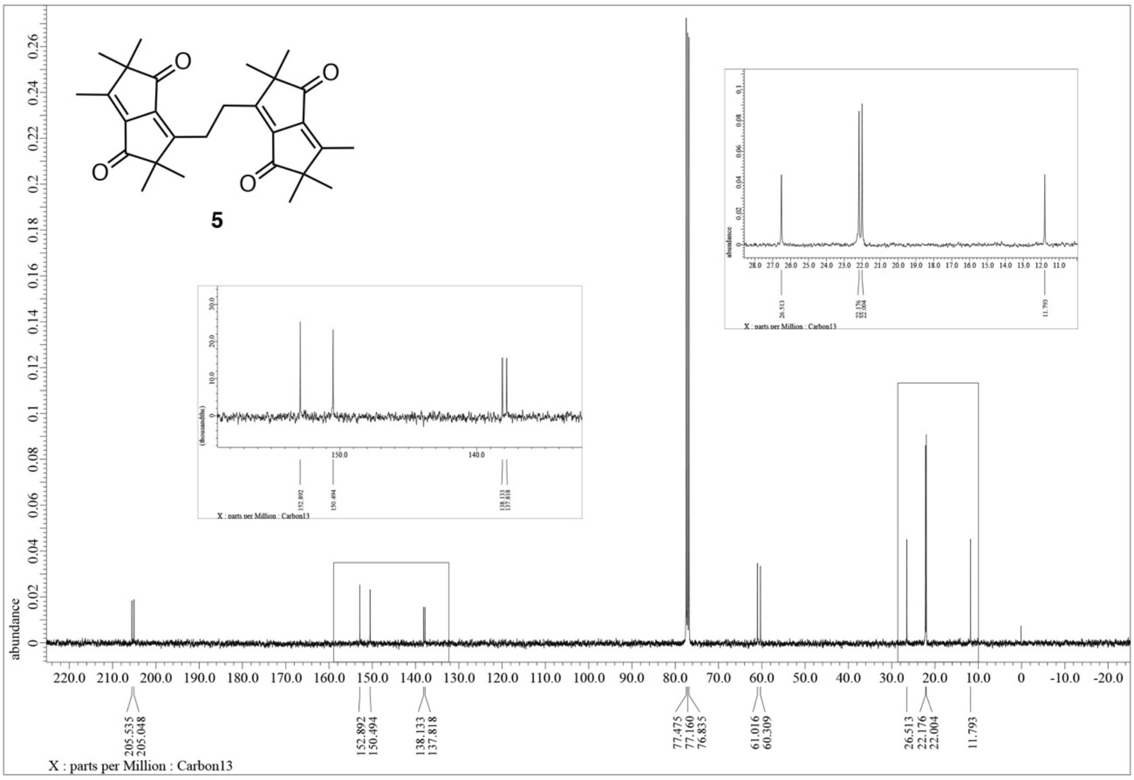

Figure S21. ^{13}C{^{1}H} NMR spectrum of compound **5** in CDCl$_3$.

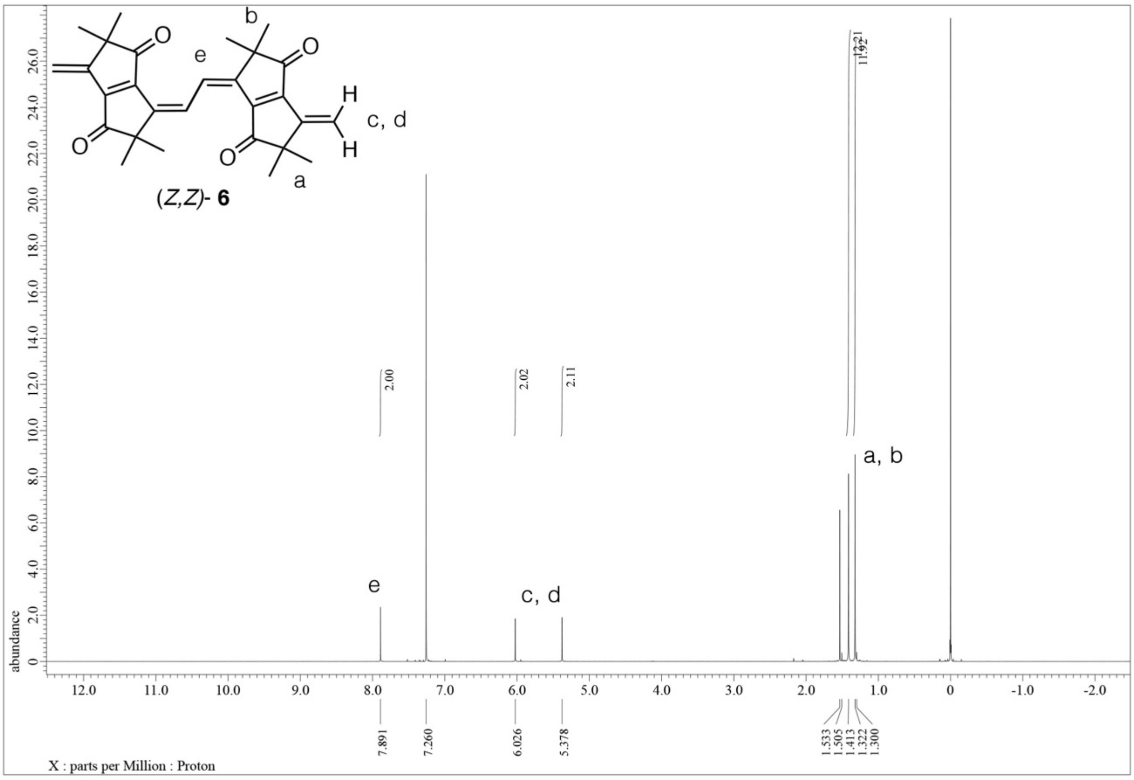

Figure S22. ^{1}H NMR spectrum of (*Z,Z*)-**6** in CDCl$_3$.

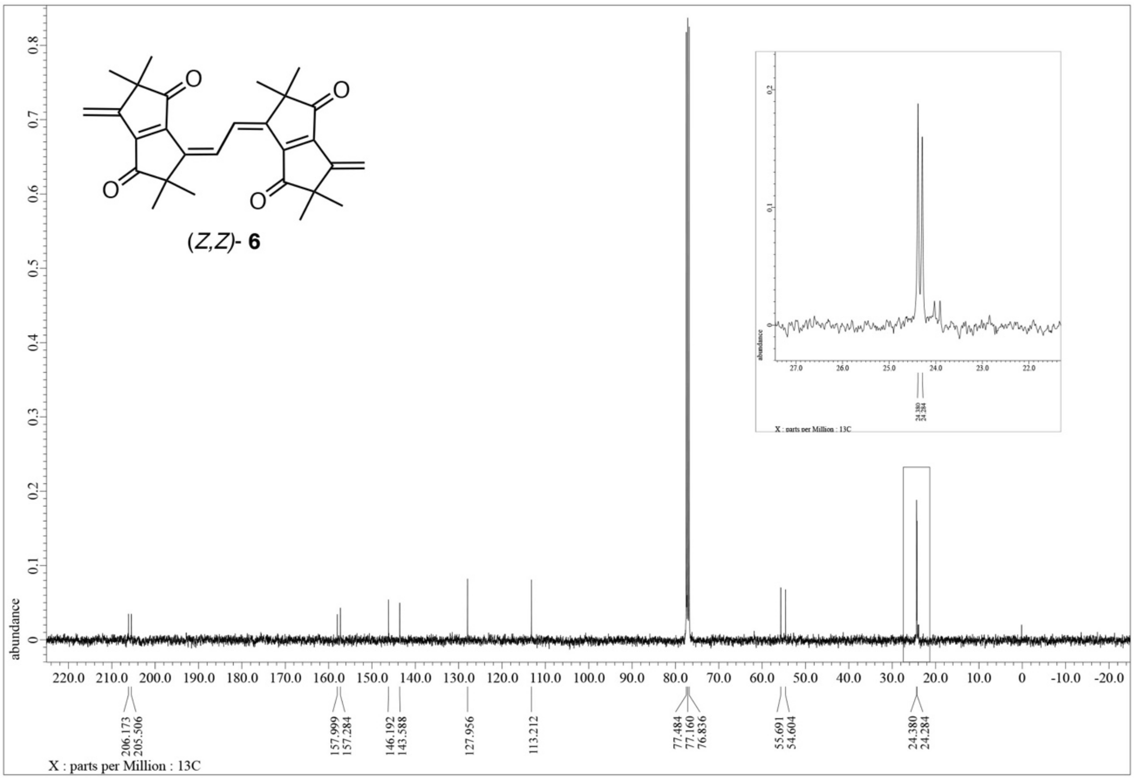

Figure S23. ^{13}C{^{1}H} NMR spectrum of (*Z,Z*)-**6** in CDCl$_3$.

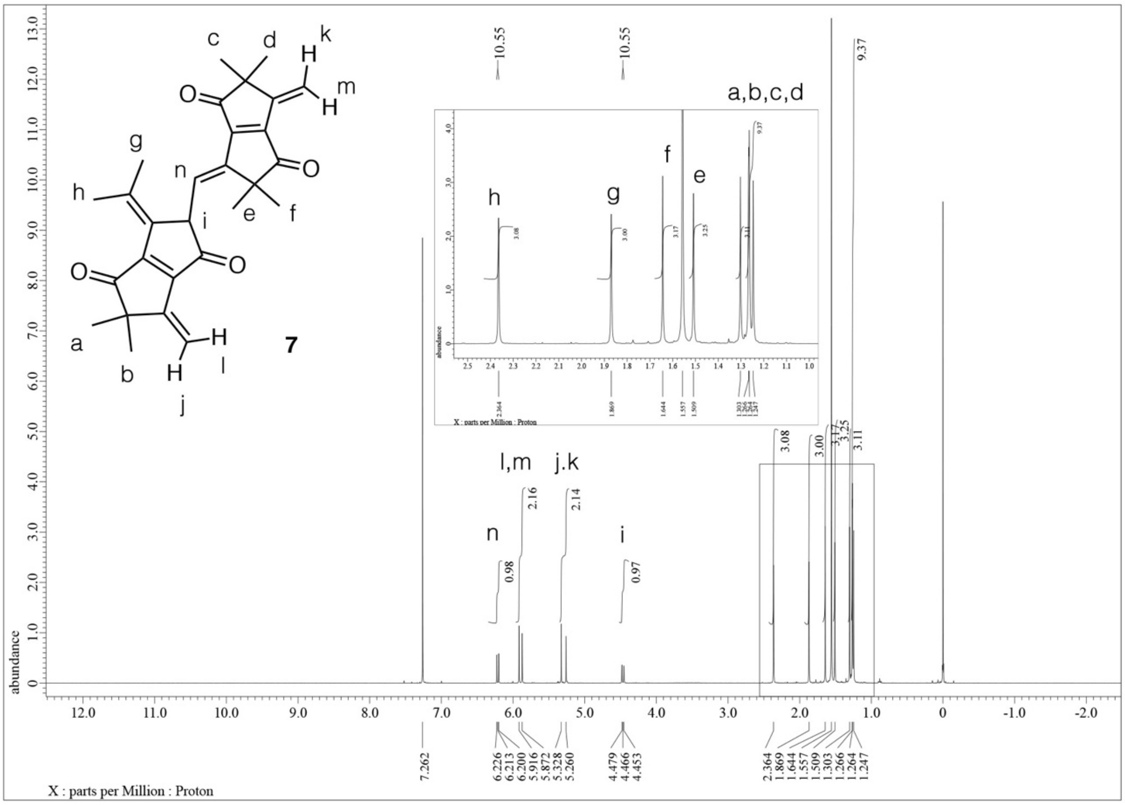

Figure S24. ^{1}H NMR spectrum of compound **7** in $CDCl_3$.

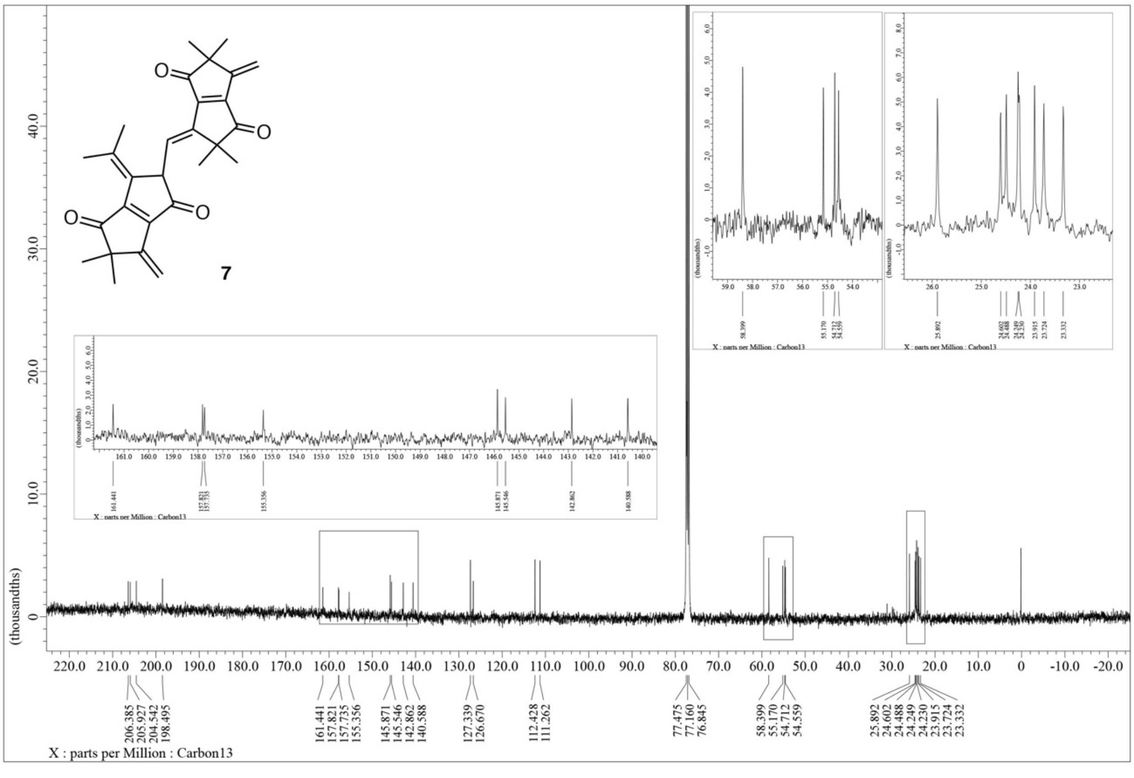

Figure S25. $^{13}C\{^{1}H\}$ NMR spectrum of compound **7** in $CDCl_3$.

VIII. Cartesian Coordinates of Optimized Structures

(*E,E*)-**6**

Total Energy = -1385.89740169 (a.u.)

O	-2.81212724	4.46953221	0.00000000
O	2.81493867	2.82554497	0.00000000
C	0.40348434	3.10262850	0.00000000
C	-0.40222491	4.20591505	0.00000000
C	1.82230158	3.53215343	0.00000000
C	-1.81419879	3.77147610	0.00000000
C	-1.81498800	2.20780594	0.00000000
C	0.33397749	5.45590412	0.00000000
C	1.82815679	5.08946259	0.00000000
C	-0.31720550	1.85372765	0.00000000
C	-0.20885401	6.68313664	0.00000000
C	-2.55548300	1.73410772	1.26999874
H	-2.01886202	2.02960851	2.17824057
H	-2.67143710	0.64640753	1.28136113
H	-3.55068488	2.18971577	1.29615769
C	0.31455752	0.64383919	0.00000000
H	1.39972030	0.68159629	0.00000000
C	2.55548300	5.58551164	-1.26606228
H	3.57395920	5.18417018	-1.28936361
H	2.60988052	6.67941309	-1.27406959
H	2.03778258	5.26569265	-2.17688597
C	-2.55548300	1.73410772	-1.26999874
H	-3.55068488	2.18971577	-1.29615769
H	-2.67143710	0.64640753	-1.28136113
H	-2.01886202	2.02960851	-2.17824057
C	2.55548300	5.58551164	1.26606228
H	2.03778258	5.26569265	2.17688597
H	2.60988052	6.67941309	1.27406959
H	3.57395920	5.18417018	1.28936361
O	2.81212724	-4.46953221	0.00000000
O	-2.81493867	-2.82554497	0.00000000
C	-0.40348434	-3.10262850	0.00000000
C	0.40222491	-4.20591505	0.00000000
C	-1.82230158	-3.53215343	0.00000000
C	1.81419879	-3.77147610	0.00000000
C	1.81498800	-2.20780594	0.00000000
C	-0.33397749	-5.45590412	0.00000000
C	-1.82815679	-5.08946259	0.00000000
C	0.31720550	-1.85372765	0.00000000
C	0.20885401	-6.68313664	0.00000000
C	2.55548300	-1.73410772	-1.26999874
H	2.01886202	-2.02960851	-2.17824057
H	2.67143710	-0.64640753	-1.28136113
H	3.55068488	-2.18971577	-1.29615769
C	-0.31455752	-0.64383919	0.00000000
H	-1.39972030	-0.68159629	0.00000000
C	-2.55548300	-5.58551164	1.26606228
H	-3.57395920	-5.18417018	1.28936361
H	-2.60988052	-6.67941309	1.27406959
H	-2.03778258	-5.26569265	2.17688597
C	2.55548300	-1.73410772	1.26999874
H	3.55068488	-2.18971577	1.29615769
H	2.67143710	-0.64640753	1.28136113
H	2.01886202	-2.02960851	2.17824057
C	-2.55548300	-5.58551164	-1.26606228
H	-2.03778258	-5.26569265	-2.17688597
H	-2.60988052	-6.67941309	-1.27406959
H	-3.57395920	-5.18417018	-1.28936361
H	1.28672108	-6.81080515	0.00000000
H	-0.40330540	-7.58083557	0.00000000
H	0.40330540	7.58083557	0.00000000
H	-1.28672108	6.81080515	0.00000000

(*E,Z*)-**6**

Total Energy = -1385.89390082 (a.u.)

O	1.61811572	5.26419852	0.00000000
O	3.22556832	-0.37565174	0.00000000
C	2.15418858	1.80831269	0.00000000
C	2.66275253	3.07769795	0.00000000
C	3.28197229	0.83820849	0.00000000
C	1.55401448	4.04720686	0.00000000
C	0.22540479	3.22497516	0.00000000
C	4.11253759	3.12558502	0.00000000
C	4.60107682	1.66920316	0.00000000
C	0.71026649	1.76021252	0.00000000
C	4.85854591	4.24104495	0.00000000
C	-0.55873483	3.61529218	1.27198890
H	-0.02368196	3.30965736	2.17763567
H	-1.54959144	3.15157432	1.29422560
H	-0.68375099	4.70279847	1.29783369
C	-0.00349716	0.59496186	0.00000000
H	0.55574518	-0.33861742	0.00000000
C	5.40894503	1.31948485	-1.26567098
H	5.61229922	0.24386492	-1.28898891
H	6.36313305	1.85749563	-1.27355297
H	4.86192121	1.58647425	-2.17643722
C	-0.55873483	3.61529218	-1.27198890
H	-0.68375099	4.70279847	-1.29783369
H	-1.54959144	3.15157432	-1.29422560
H	-0.02368196	3.30965736	-2.17763567
C	5.40894503	1.31948485	1.26567098
H	4.86192121	1.58647425	2.17643722
H	6.36313305	1.85749563	1.27355297
H	5.61229922	0.24386492	1.28898891
O	-5.34147832	-2.43234337	0.00000000
O	0.53206389	-2.52433579	0.00000000
C	-1.85619121	-2.01350788	0.00000000
C	-2.95295954	-2.83667987	0.00000000
C	-0.63430526	-2.86869871	0.00000000
C	-4.18982163	-2.03319083	0.00000000
C	-3.75609068	-0.54451172	0.00000000
C	-2.63219146	-4.24940058	0.00000000
C	-1.10291090	-4.35264500	0.00000000
C	-2.21601024	-0.60826389	0.00000000
C	-3.52603534	-5.25076042	0.00000000
C	-4.31967490	0.13378231	1.26622481
H	-3.90781191	-0.31369785	2.17721806
H	-4.08115258	1.20291504	1.27484590
H	-5.40849910	0.02032491	1.28869626
C	-1.43801394	0.51182983	0.00000000
H	-1.97884561	1.45385825	0.00000000
C	-0.55873483	-5.04501891	-1.26606842
H	0.53314341	-4.96935990	-1.28863441
H	-0.83797973	-6.10413259	-1.27306092
H	-0.95565016	-4.58372170	-2.17688963
C	-4.31967490	0.13378231	-1.26622481
H	-5.40849910	0.02032491	-1.28869626
H	-4.08115258	1.20291504	-1.27484590
H	-3.90781191	-0.31369785	-2.17721806
C	-0.55873483	-5.04501891	1.26606842
H	-0.95565016	-4.58372170	2.17688963
H	-0.83797973	-6.10413259	1.27306092
H	0.53314341	-4.96935990	1.28863441
H	-4.59091850	-5.04147855	0.00000000
H	-3.21816860	-6.29281979	0.00000000
H	5.94448220	4.20328029	0.00000000
H	4.39079177	5.22048763	0.00000000

(*Z,Z*)-**6**

Total Energy = -1385.90060256 (a.u.)

O	5.47908573	0.30007534	0.00000000
O	0.77696567	-3.22784524	0.00000000
C	2.40664240	-1.39995708	0.00000000
C	3.77862220	-1.42375297	0.00000000
C	1.92275917	-2.81001300	0.00000000
C	4.31005340	-0.04579050	0.00000000
C	3.08759845	0.90481018	0.00000000
C	4.34959998	-2.75439749	0.00000000
C	3.17268927	-3.73575355	0.00000000
C	1.87760299	-0.04723899	0.00000000
C	5.66096363	-3.04094875	0.00000000
C	3.13871107	1.78722584	1.26538148
H	3.07549553	1.18303071	2.17711846
H	2.30847360	2.50090141	1.26964192
H	4.08168667	2.34345780	1.28607290
C	0.59184329	0.40583233	0.00000000
H	0.44463324	1.48300955	0.00000000
C	3.13871107	-4.61565074	-1.26615623
H	2.21099177	-5.19647026	-1.28924888
H	3.98663242	-5.30879469	-1.27307296
H	3.18964774	-4.00887925	-2.17668533
C	3.13871107	1.78722584	-1.26538148
H	4.08168667	2.34345780	-1.28607290
H	2.30847360	2.50090141	-1.26964192
H	3.07549553	1.18303071	-2.17711846
C	3.13871107	-4.61565074	1.26615623
H	3.18964774	-4.00887925	2.17668533
H	3.98663242	-5.30879469	1.27307296
H	2.21099177	-5.19647026	1.28924888
O	-5.47908573	-0.30007534	0.00000000
O	-0.77696567	3.22784524	0.00000000
C	-2.40664240	1.39995708	0.00000000
C	-3.77862220	1.42375297	0.00000000
C	-1.92275917	2.81001300	0.00000000
C	-4.31005340	0.04579050	0.00000000
C	-3.08759845	-0.90481018	0.00000000
C	-4.34959998	2.75439749	0.00000000
C	-3.17268927	3.73575355	0.00000000
C	-1.87760299	0.04723899	0.00000000
C	-5.66096363	3.04094875	0.00000000
C	-3.13871107	-1.78722584	-1.26538148
H	-3.07549553	-1.18303071	-2.17711846
H	-2.30847360	-2.50090141	-1.26964192
H	-4.08168667	-2.34345780	-1.28607290
C	-0.59184329	-0.40583233	0.00000000
H	-0.44463324	-1.48300955	0.00000000
C	-3.13871107	4.61565074	1.26615623
H	-2.21099177	5.19647026	1.28924888
H	-3.98663242	5.30879469	1.27307296
H	-3.18964774	4.00887925	2.17668533
C	-3.13871107	-1.78722584	1.26538148
H	-4.08168667	-2.34345780	1.28607290
H	-2.30847360	-2.50090141	1.26964192
H	-3.07549553	-1.18303071	2.17711846
C	-3.13871107	4.61565074	-1.26615623
H	-3.18964774	4.00887925	-2.17668533
H	-3.98663242	5.30879469	-1.27307296
H	-2.21099177	5.19647026	-1.28924888
H	-6.39978900	2.24612071	0.00000000
H	-6.02345248	4.06527126	0.00000000
H	6.02345248	-4.06527126	0.00000000
H	6.39978900	-2.24612071	0.00000000

Compound **3**

Total Energy = -693.24670802 (a.u.)

C	1.35551673	-1.21906798	-0.04848229
C	-0.02714811	-0.67669352	-0.00046265
C	-1.38280072	-1.19892643	0.03264012
C	-2.31772127	0.01470615	-0.02477543
C	-1.73904892	-2.47984742	0.11260663
H	-1.07285971	-3.15669403	0.15552052
H	-2.65862606	-2.71756940	0.12794087
C	-3.06549027	0.08012375	-1.36915784
H	-3.66481851	-0.69109704	-1.44778453
H	-2.41745882	0.06689226	-2.10382113
H	-3.58919086	0.90777187	-1.41069451
C	-3.31272567	0.06044274	1.13747902
H	-2.82465197	0.04256191	1.98739039
H	-3.90912037	-0.71596854	1.08915832
H	-3.84208605	0.88284030	1.08232623
O	1.68701173	-2.38262693	-0.14710596
C	-1.35551673	1.21906798	0.04848229
C	0.02714811	0.67669352	0.00046265
C	1.38280072	1.19892643	-0.03264012
C	2.31772127	-0.01470615	0.02477543
C	1.73904892	2.47984742	-0.11260663
H	1.07285971	3.15669403	-0.15552052
H	2.65862606	2.71756940	-0.12794087
C	3.06549027	-0.08012375	1.36915784
H	3.66481851	0.69109704	1.44778453
H	2.41745882	-0.06689226	2.10382113
H	3.58919086	-0.90777187	1.41069451
C	3.31272567	-0.06044274	-1.13747902
H	2.82465197	-0.04256191	-1.98739039
H	3.90912037	0.71596854	-1.08915832
H	3.84208605	-0.88284030	-1.08232623
O	-1.68701173	2.38262693	0.14710596

Compound **7**

Total Energy = -1385.92747870 (a.u.)

C	3.70411600	-1.75225400	-0.27305500
C	2.17141400	-2.04261900	-0.17881900
C	1.55252100	-0.63969500	0.00076000
C	2.65688000	0.30257600	-0.07704500
C	2.82855400	1.77379500	-0.02226900
C	4.35037500	2.06384100	-0.18157900
C	4.97304600	0.66333500	-0.30407400
C	3.87528800	-0.28582200	-0.23275200
C	1.75320800	-2.70803500	-1.50994100
H	2.33605800	-3.62313200	-1.65196300
H	1.94093300	-2.04391500	-2.35887400
H	0.68819500	-2.94516900	-1.51793200
C	1.94194200	-3.00541300	1.00164800
H	0.90776100	-3.35929100	1.03988800
H	2.18221000	-2.53388100	1.95976400
H	2.59307400	-3.87587100	0.88023500
C	4.56378000	2.91287000	-1.45104600
H	3.99284800	3.84293200	-1.37450600
H	4.23536100	2.37988100	-2.34855200
H	5.62261000	3.16052900	-1.57277300
C	4.84740300	2.82515300	1.06302700
H	4.73217000	2.22549300	1.97116500
H	4.27311800	3.74821900	1.18442300
H	5.90589800	3.08210300	0.95922700
C	6.26873100	0.35122900	-0.44840900
H	6.58083100	-0.68492100	-0.52267900
H	7.03907200	1.11503100	-0.49482100
C	0.28290400	-0.22520400	0.19836700
H	0.13696600	0.85042500	0.27818400
C	-0.97867100	-1.04433900	0.29077900
H	-0.75192000	-2.08877500	0.52587000
C	-1.70883700	-1.03183000	-1.08697800
C	-2.98249100	-0.33260600	-0.86831500
C	-4.08133300	0.05921100	-1.72826700
C	-5.10255500	0.75763600	-0.83039200
C	-4.45850100	0.69173500	0.58270500
C	-3.14051700	-0.01108400	0.45450500
C	-2.00946100	-0.44744300	1.27666700
C	-4.15982400	-0.16229700	-3.04843600
H	-3.36023200	-0.67667100	-3.56982800
H	-5.01754900	0.16126200	-3.63014100
C	-6.45606100	0.01936900	-0.78950400
H	-7.10017600	0.47091100	-0.02962400
H	-6.32660900	-1.04015000	-0.54830300
H	-6.95708400	0.08690100	-1.75974600
C	-5.31002800	2.23738200	-1.21192000
H	-4.35720400	2.77187100	-1.27242700
H	-5.93476900	2.72861800	-0.46056100
H	-5.80450800	2.31409300	-2.18482100
C	-1.84117800	-0.39406800	2.62193000
C	-2.84102000	0.17963900	3.58791100
H	-3.72141600	0.60220900	3.10837900
H	-2.36062100	0.96023400	4.19253500
H	-3.15926900	-0.59783300	4.29553400
C	-0.60747000	-0.93914000	3.29489400
H	-0.89040700	-1.70755800	4.02601100
H	-0.10841900	-0.14484200	3.86459800
H	0.12003600	-1.36684100	2.60805100
O	-1.29141100	-1.51448900	-2.12337800
O	-4.99218600	1.15818700	1.57271800
O	1.96544500	2.62157800	0.12164800
O	4.56937100	-2.60369900	-0.36832100

IX. References

[1] M. Uesaka, Y. Saito, S. Yoshioka, Y. Domoto, M. Fujita, Y. Inokuma, *Commun. Chem.*, 2018, **1**, 23.

[2] Y. Saito, M. Higuchi, S. Yoshioka, H. Senboku, Y. Inokuma, *Chem. Commun.,* 2018, **54**, 6788–6791.

[3] Gaussian 09, Revision A.02, M. J. Frisch, G. W. Trucks, H. B. Schlegel, G. E. Scuseria, M. A. Robb, J. R. Cheeseman, G. Scalmani, V. Barone, G. A. Petersson, H. Nakatsuji, X. Li, M. Caricato, A. Marenich, J. Bloino, B. G. Janesko, R. Gomperts, B. Mennucci, H. P. Hratchian, J. V. Ortiz, A. F. Izmaylov, J. L. Sonnenberg, D. Williams-Young, F. Ding, F. Lipparini, F. Egidi, J. Goings, B. Peng, A. Petrone, T. Henderson, D. Ranasinghe, V. G. Zakrzewski, J. Gao, N. Rega, G. Zheng, W. Liang, M. Hada, M. Ehara, K. Toyota, R. Fukuda, J. Hasegawa, M. Ishida, T. Nakajima, Y. Honda, O. Kitao, H. Nakai, T. Vreven, K. Throssell, J. A. Montgomery, Jr., J. E. Peralta, F. Ogliaro, M. Bearpark, J. J. Heyd, E. Brothers, K. N. Kudin, V. N. Staroverov, T. Keith, R. Kobayashi, J. Normand, K. Raghavachari, A. Rendell, J. C. Burant, S. S. Iyengar, J. Tomasi, M. Cossi, J. M. Millam, M. Klene, C. Adamo, R. Cammi, J. W. Ochterski, R. L. Martin, K. Morokuma, O. Farkas, J. B. Foresman, and D. J. Fox, Gaussian, Inc., Wallingford CT, 2016.

[4] G. M. Sheldrick, *Acta Crystallogr. Sect. A*, 2015, **71**, 3–8.

[5] G. M. Sheldrick, *Acta Crystallogr. Sect. C*, 2015, **71**, 3–8.

[6] F. C. Spano, *J. Chem. Phys.* 2002, **116**, 5877-5891.

[7] F. C. Spano, *Acc. Chem. Res.* 2010, **43**, 429-439.

[8] K. Miyata, S. Tanaka, Y. Ishino, K. Watanabe, T. Uemura, J. Takeya, T. Sugimoto, and Y. Matsumoto, *Phys. Rev.* B 2015, **91**, 195306.